

Internship report

Enhancement of geodata: The assessment of a near-infrared UAV sensor and a performance study of a low-cost dual-frequency GNSS receiver



AUTHOR

Myke Koopmans

DATE

April 2020

Enhancement of geodata: The assessment of a near-infrared UAV sensor and a performance study of a low-cost dual-frequency GNSS receiver

Internship report

Author

Myke Koopmans

Supervisors

Corjan Nolet (FutureWater)

Lammert Kooistra (Wageningen University)

Date

April 2020

FutureWater

ADDRESS

FutureWater B.V.
Costerweg 1V
6702 AA Wageningen
The Netherlands

TELEPHONE

+31 317 460 050

WEBSITE

www.futurewater.eu

Summary

The accuracy and consistency of geodata are important elements for reliable geo-information. This report will focus on two components related to the reliability of geodata. The first component will address reliability of the UAV data of the MAPIR Survey 3 sensor. The second will focus on improving location accuracy of geodata with the use of the ArduSimpleRTK2B system.

The data of the MAPIR Survey 3 sensor gave unrealistically low NDVI values. The data was assessed by analysing the reflectance histograms of non-calibrated and calibrated images. This showed an unexpected response, namely the bands used for the NDVI calculations, the Orange and Near infrared bands showed a very comparable response in both the non-calibrated and calibrated images. In addition, the MAPIR data was compared to satellite data, Landsat 8 and Sentinel-2A, in order to assess the possibility of developing a correction factor for the NDVI values of the MAPIR data. There was no clear correlation between the two data sources, indicating that satellite data is not an appropriate source to develop a correction factor with.

The ArduSimpleRTK2B system was assessed on its location accuracy and its ability to improve the comparability of geodata. The ArduSimpleRTK2B system is a low-cost Real Time Kinematic (RTK) system. The system was compared to the Topcon V, an established RTK system with an accuracy of 2cm. This showed promising results with an average difference of 1.1 cm in X-direction, 2.6 cm in Y-direction and 6cm in elevation. The ArduSimple base station is able to determine its own location, where the accuracy of this determination will increase with time. However, the system will be more accurate when the base stations is provided with a known surveyed location.

Content

Summary	3
1 Introduction	7
1.1 Internship organisation background	7
1.2 Context and justification of research	7
1.2.1 Context	7
1.2.2 The significance of this topic	7
1.3 Research aim and objectives	11
2 The concept of GNSS and RTK	12
2.1 GNSS	12
2.2 RTK	12
2.3 GNSS error sources	13
2.3.1 Clock related errors	13
2.3.2 Signal propagation errors	14
2.3.3 System errors	14
2.4 GNSS height determination	14
3 Methodology	16
3.1 MAPIR	16
3.1.1 Raw vs. calibrated data	16
3.1.2 Satellite comparison	17
3.2 The ArduSimple RTK System	18
3.2.1 Test 1	19
3.2.2 Test 2	19
3.2.3 Test 3	19
4 Results and discussion	22
4.1 MAPIR image analysis	22
4.1.1 Reflective histograms	22
4.1.2 Comparison with satellite data	25
4.1.3 General performance	26
4.2 The ArduSimple RTK system	27
4.2.1 Test 1	27
4.2.2 Test 2	28
4.2.3 Test 3	30
4.2.4 General performance	32
5 Conclusion	34
6 Recommendations	35
References	36
Annex I	39
Annex II	43
Annex III	47

7	User guide ArduSimple RTK System with WiFi connection	50
7.1	Necessary material	50
7.2	The RTK principle	50
7.3	Base station	50
7.4	Base station set-up	51
7.5	U-center settings	52
7.6	NTRIP network	55
7.7	Rover	56
	7.7.1 Rover set-up	56
	7.7.2 Mobile phone	57
	7.7.3 Laptop	60
7.8	Height in GNSS	61
7.9	Using an external base station	62
7.10	Changes in the configurations	63

Tables

Table 1 An overview of the settings during the different sets of measurements	20
Table 2 The R-RMSE (in %) for each band of the selected areas for each location.....	25
Table 3 The comparison between the measurement differences on the U-Shaped hill of the ArduSimple RTK and the Topcon V RTK system.	27
Table 4 Result test 2, time measurements	29
Table 5 An overview of the compared sets.....	30
Table 6 Line distance information of the compared to sets.....	31
Table 7 The difference in X direction of the compared to sets.....	31
Table 8 The difference in Y direction of the compared to sets.....	31
Table 9 The difference in Z direction of the compared to sets.....	31

Figures

Figure 1 The difference in reflection of near infrared and visible red light for healthy (left) and unhealthy (right) vegetation. Source: Weier and Herring, 2020.....	8
Figure 2 The transmission of light of the MAPIR Survey 3 OCN filter. Source: MAPIR, 2020a.	9
Figure 3 A visual representation on how a GNSS receivers' position is determined. Source: Teunissen and Montenbruck, 2017	12
Figure 4 The principle of RTK, where A is the base station and B the rover station. Source: Drotek, 2020.....	13
Figure 5 A schematic overview of the geoid height (N), the orthometric height (H) and the ellipsoidal height (h). Source: unavco, 2020.....	15
Figure 6 The schematic setup of the base station (A), and the rover station (B)	18
Figure 7 The sampled locations on the U-shaped hill at the Wageningen University campus.....	19
Figure 8 The location of the RD-point on the 'Ginkelse hei' near the town of Ede.	21
Figure 9 The reflectance histogram of the raw image with the land use of Rapini in the USA.....	22
Figure 10 The reflectance histogram of the processed image with the land use of Rapini in the USA .	22
Figure 11 RTK setup, where A is the base station and B is the rover station.	50
Figure 12 A schematic overview of the geoid height (N), the orthometric height (H) and the ellipsoidal height (h). Source: unavco, 2020.....	61

1 Introduction

1.1 Internship organisation background

The internship will be conducted at FutureWater. FutureWater is a research and consultancy company. Their main objective is to contribute to the sustainable management of water resources. FutureWater focuses on the application and development of scientific methods and concepts to provide advice and practical solutions in the field of water management. The company works at global, national and local levels. They work with governments, river basin authorities, and NGOs. Important topics are water for food, irrigation, water excess, water shortage, climate change, and river basin management. FutureWater's key expertise is in the field of quantitative methods, based on simulation models, geographic information systems and satellite observations.

The internship will be part of Horizon 2020 project TWIGA: Transforming Weather Water data into value-added Information services for sustainable growth in Africa. This project aims to provide geo-information on weather, water, and climate in Africa through innovative combinations of new in situ sensors and satellite-based geo-data. The main role of FutureWater in the TWIGA project relates to the use of flying sensors to map crop conditions, flood extent, and energy fluxes, complementing and improving data from in situ sensors and satellites (FutureWater, 2020).

1.2 Context and justification of research

1.2.1 Context

Climate change has an influence on crop production. The change in temperature and precipitation, as well as the occurrence of extreme events like droughts and floods, can significantly affect crop yields. In addition, the changing climate can also affect the occurrence of pests and diseases within the crops (Landi and Benelli., 2016). Geoinformation can play a role in the mitigation of these climate change effect. Remote sensing can, for instance, be a useful tool to monitor crop conditions. The vegetation can be monitored based on the spectral reflectance of the plant. When the crop is under stress, for instance, due to a lack of water or a disease, this spectral reflectance will change (Mutanga et al., 2017). Crop conditions are often expressed through vegetation indices. The indices can help in the assessment of plant stress, water use, biomass and crop production (Xue and Su, 2017; Jackson and Heurte, 1991).

Sub-Saharan Africa is a region that could benefit from reliable and detailed geo-information. It is predicted that climate change will have large impacts on the region. Predicted warmer and drier conditions will have large impacts on agricultural activities in the region. These changes in weather conditions will affect the duration of the growing season, the suitable areas for agriculture and the yield potential (IPPC, 2007). In addition, food demands are expected to increase drastically in this area (van Ittersum et al., 2016). Reliable and detailed geoinformation can help farmers and policymakers to adapt to and cope with the impacts of the changing climate.

1.2.2 The significance of this topic

The accuracy and consistency of geodata are important elements for reliable geo-information. These two elements are also influential for the comparison of data. This comparison can be between data from the same source or between different sources (e.g. the comparison of satellite data with UAV data). This research will focus on two components related to the reliability of geodata. The first component will address the reliability of the UAV data of the MAPIR Survey 3 sensor. The second will focus on improving location accuracy of geodata with the use of the ArduSimpleRTK2B system.

MAPIR Survey 3 sensor

FutureWater has a UAV equipped with a MAPIR Survey 3 sensor. One of the purposes of this sensor is to be able to make detailed NDVI calculations. The Normalized Differenced Vegetation Index (NDVI) is a widely used vegetation index. This index uses near-infrared (which vegetation reflects) and red light (which vegetation absorbs). Healthy vegetation absorbs more of the red light and reflects a larger portion of the near infrared compared to unhealthy or less vegetation (Fig 1). With the vegetation indices, it is possible to make comparisons of vegetation over time and between locations. In order to make a good comparison, it is important that there is reliable geodata. Satellite data is often too coarse when doing analysis on field level, especially when the dimensions of the field are in the order of meters. The usage of unmanned aerial vehicles (UAVs) enables the acquisition of higher resolution geodata and the usage is relatively flexible (Barbedo, 2019).

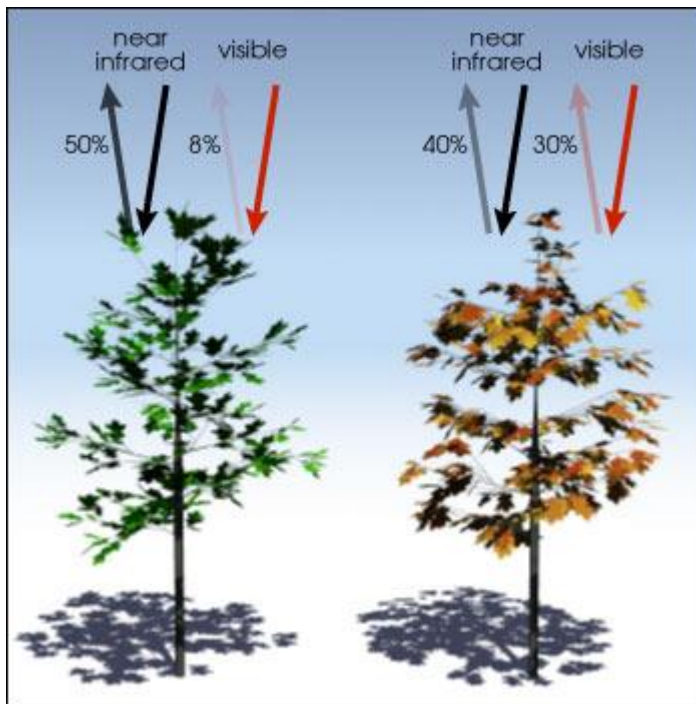


Figure 1 The difference in reflection of near infrared and visible red light for healthy (left) and unhealthy (right) vegetation. Source: Weier and Herring, 2020

The MAPIR Survey 3 sensor has an OCN (Orange/Cyan/Near-infrared) filter. This filter captures orange at 615nm, cyan at 490nm and near-infrared at 808nm. MAPIR aimed, with the shift to capture orange instead of red light, to reduce the pixel noise caused by high red reflectance of soil when capturing areas with soil. It should therefore be possible to get a higher level of contrast in the NDVI (MAPIR, 2020a). The transmission of light of sensors OCN filter can be seen in Figure 2.

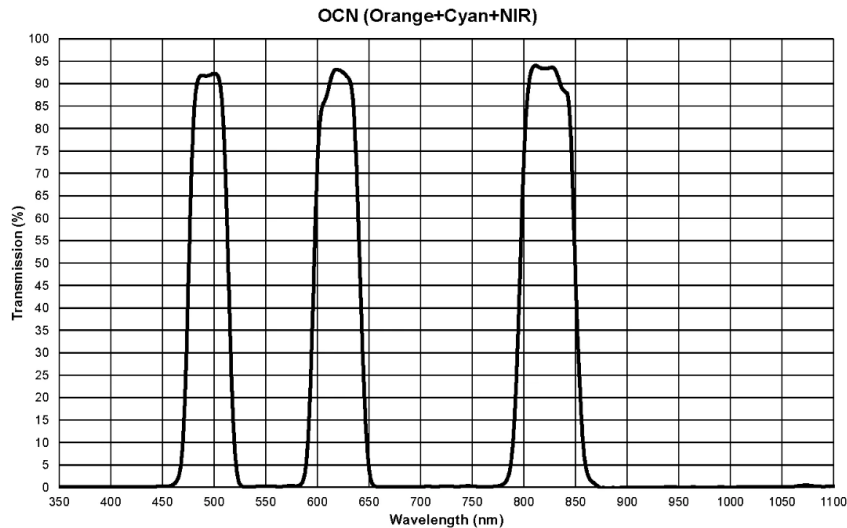


Figure 2 The transmission of light of the MAPIR Survey 3 OCN filter. Source: MAPIR, 2020a.

The NDVI contrast differences between using an RGN (red/green/near-infrared) filter and OCN filter are shown in Figure 3 (MAPIR, 2020a). In this figure the NDVI patterns are compared between an RGN and an OCN image, the RGB image is the reference image which depicts the real situation. In the RGN image, the red areas, which indicate soil, are almost always surrounded by yellow areas. In the OCN image, the transition between soil and vegetation is more defined. In addition, smaller sections of vegetation are also captured in the OCN image where this is not in the RGN image due to the pixel noise, even though the pixel size is the same. This shows the advantages of using the MAPIR OCN data. However, the NDVI values calculated based on FutureWater's UAV data with the OCN filter were much lower than expected. The NDVI is normally calculated with red and near-infrared, with the following formula (Rouse et al., 1974):

$$NDVI = \frac{NIR-Red}{NIR+Red} \quad \text{(Equation 1)}$$

When using the MAPIR OCN data, the NDVI is calculated based on the Orange and NIR bands (MAPIR, 2020a). These MAPIR NDVI values were especially low for vegetation; NDVI values ranging between 0.1 and 0.15 where 0.8-0.9 was expected. The NDVI values for bare soil, buildings, water, etc. were as expected. As a result, these low NDVI values for vegetated areas are not representative of the status of the vegetation and become incomparable to other (spectral reflectance data) sources. Therefore, there

is a need to assess the reasons behind the unrealistically low NDVI values of the MAPIR Survey 3 sensor data in order to use the data for vegetation monitoring.

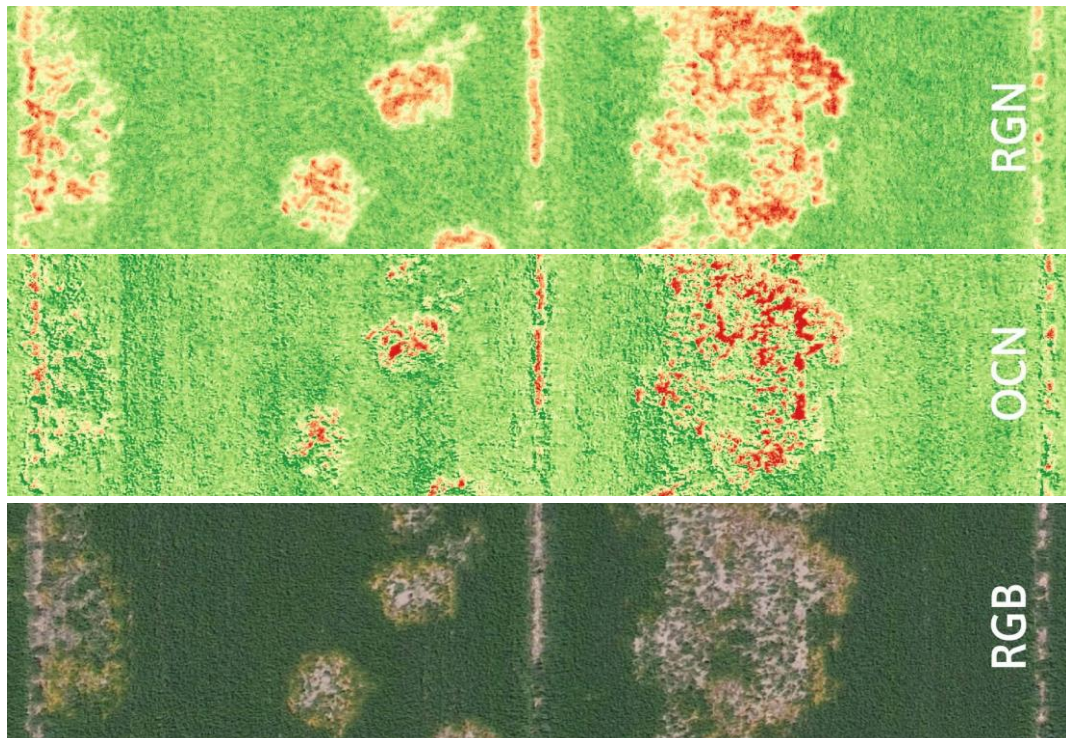


Figure 3 A pattern comparison of the difference in contrast when using an RGN filter compared to the OCN filter. Source: MAPIR, 2020a

The ArduSimpleRTK2B system

A high degree of global accuracy could help to improve the comparability of data. The usage of ground control points (GCP) can greatly improve the global accuracy of UAV data. GCPs are clearly identifiable objects within the images with known coordinates. These points and their known locations will be linked to the UAV image to improve the data's position accuracy. It is important to use a system which can determine the accurate locations of the GCP (Sanz-Ablanedo et al., 2018; Rieke et al., 2011). Often Real Time Kinematic (RTK) systems are used for this. The RTK technology enables high accuracy in real-time (Saghravani et al., 2009). This is reached by measuring the signal from the same satellite by at least two receivers. One of the receivers has a fixed location; 'the base station'. The other receiver, 'the rover', can be a moving object. The rover receives messages from the base station regarding the differences between both points (Pirti et al., 2013).

However, these RTK systems usually come with high investment cost. This research will assess the performance of a low-cost dual-frequency GNSS receiver to improve the location accuracy of the data. Within this research, the ArduSimpleRTK2B system (ArduSimple, 2020) will be assessed on its location accuracy and its ability to improve the comparability of geodata. The ArduSimpleRTK2b is an Arduino application board that makes it possible to have a fast evaluation of dual-band GNSS technology including RTK functionality. The ArduSimpleRTK system can provide cm accuracy, comparable to high-end GNSS RTK devices. Besides its considerably lower investment cost, the system is easy to transport due to its compact size.

1.3 Research aim and objectives

The main objective of this study is to improve the accuracy and consistency of FutureWater`s geodata to enable and improve the comparison of data in time and between multiple locations. This will also help to improve the integration of the geodata with other techniques, for instance, satellite remote sensing.

The following sub-objectives are set up to address the main research objective:

- Objective 1: Perform a quality assessment for the MAPIR Survey 3 sensor data in order to assess the reasons behind the unrealistically low NDVI values.
- Objective 3: Develop a correction factor based on the insights gained from the quality assessment to be able to compute realistic NDVI values from the MAPIR Survey 3 sensor data.
- Objective 3: Get the ArduSimple RTK system operating and assess the usability of the system.
- Objective 4: Compare the location accuracy of the ArduSimple RTK system to an established RTK system to determine its performance.

2 The concept of GNSS and RTK

2.1 GNSS

Global Navigation Satellite Systems (GNSS) comprise of a large number of satellites orbiting the earth. GNSS is a generic name for any global navigation satellite system; this includes GPS (USA), Galileo (EU), Glonass (RUS), and BeiDou (CHN). These systems are used to determine a user's position on earth. This is done by measuring the distance between a receiver and several satellites. GNSS satellites send a signal in all directions. This signal consists of three elements, namely a carrier wave, spreading code and navigation data. The satellite orbit and clock information are included in the navigation data. The navigation data and spreading code send on the carrier wave. Each satellite has unique Pseudo Random Noise (PRN) on the carrier wave, whereby it can be identified. A receiver obtains this PRN signal. The travel time between the satellite and the receiver is determined through the shift in time of the PRN code, this is also referred to as pseudorange code measurements. The travel time is multiplied with the speed of light to calculate the range distance. The calculated range equals to a radius of a sphere which is centred on a satellite. A receiver's position is determined by the point on earth where multiple of these circles meet (Fig. 3). To improve the accuracy of the measurement, a carrier phase measurement is used. With this technique also the distance between the receiver and the satellite is determined, however here it is done with the carrier wave (Teunissen and Montenbruck, 2017).

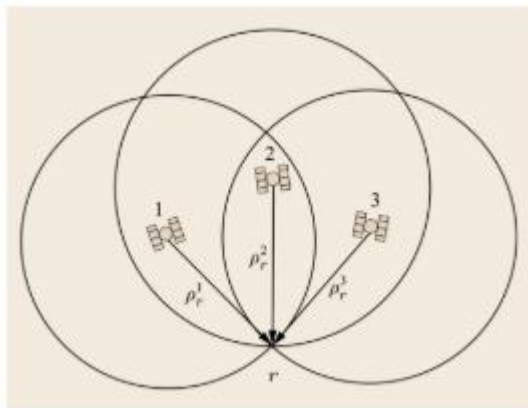


Figure 3 A visual representation on how a GNSS receivers' position is determined. Source: Teunissen and Montenbruck, 2017

2.2 RTK

The RTK technology consists of at least two GNSS receivers. One receiver is located at a known location, this is referred to as the base station. The other receiver(s), the rover, is used to determine an unknown position. The rover can be used in a static or mobile state. The system provides real-time correction, which enables up to centimetre-level accuracy (Pirti et al., 2013; Xu, 2012). The RTK system has two types of accuracy statuses: the float and fix solution. The float solution requires at least four common satellites and provides an accuracy ranging between 20cm and 1m. The fix solution needs at least five common satellites, which will offer a within 2cm accuracy (Xu, 2012).

The basic setup of an RTK system can be seen in Figure 4. The base station sends correction data to the rover. The corrections are based on the difference between the known location of the base station and the location which is calculated by the base station based on the satellite connections at that moment. The idea is that the rover station will have the same error sources as the base stations, which will therefore be corrected for the rover's position (Xu, 2012). The GNSS errors will be more similar if the baseline, the distance between the base station and the rover, is smaller. Within the RTK there will not

be corrected for multipath and receiver noise errors. More information on GNSS errors can be found in the next sub-chapter.

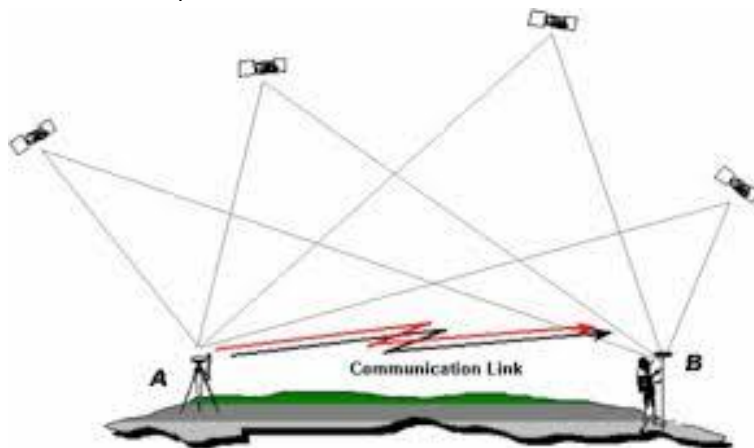


Figure 4 The principle of RTK, where A is the base station and B the rover station. Source: Drotek, 2020

The data transfer between the base station and the rover can be established via different media. The real-time data transmission can be via radio or via an internet connection (Bakula et al., 2009; Pirti et al., 2013; Xu, 2012). This study will focus on the internet connection. The Network Transport of RTCM via Internet Protocol (NTRIP) will be used to provide an online connection between the rover and the base station (Uradzinski et al., 2008).

2.3 GNSS error sources

GNSS errors can have a variety of sources. In this chapter the errors will be described according to their origin. The main sources of errors which will be discussed in this chapter are: Clock related errors, Signal propagation errors, and system errors.

2.3.1 Clock related errors

Timing is an important element in a GNSS system. The drift in time can translate in large errors of the receiver measurements. Clock related errors can be caused by satellite clock errors, receiver clock errors, and intersystem biases (Karaim et al., 2018). There are two main factors which affect satellite clock errors. The first factor is clock stability. A satellite clock contains an atomic clock, these clocks are highly stable however they have still some instability (Bibikar et al., 2014). Which ranges for a satellite clock from 8.64 to 17.28ns a day. This equals to a range error of 2.59 to 5.18m (El-Rabbany, 2002). The second factor is the relativistic effects. A clock on board of a satellite will appear to run faster compared to the same clock on earth. Before the launch of a satellite, an offset will be made to the satellite's clock in order to compensate for these relativistic effects. However, due to the noncircular orbit of the satellites there is still a small effect (Ashby, 1995; Karaim et al., 2018).

Receiver clock errors are usually much larger than satellite clock errors. This is the result of the usage of less expensive clocks, which are less accurate compared to the clocks used in the satellites (Karaim et al., 2018; Pratt et al., 2013).

The usage of multiple GNSS constellations (e.g. GPS, GLONASS, Galileo and BeiDuo) is a way to improve the accuracy and the availability of receiver solution. However, each system has its own timing system. These inter-system clock biases should be taken into account when working with multi-GNSS constellations (Karaim et al., 2018).

2.3.2 Signal propagation errors

The error sources which are in the group of signal propagation errors and which will be discussed are the Sagnac effect, Ionospheric error, Tropospheric error, and multipath error. The Sagnac effect is the error caused by the earth's rotation during the moment the satellite transmit its signal and the moment the receiver receives the signal. This can result in an additional error in the measured range, when not accounted for this effect (Kaplan and Hegarty, 2005; Ashby, 1995).

The ionospheric errors are errors which have an origin in the ionosphere, the upper layer of the atmosphere at an altitude of about 1000km above the earth's surface. The reflective properties in this layer can influence the transmitted signal from the satellite. The solar activity, time of day and the season are the key factors in determining the ionospheric conditions and thereby the magnitude of the errors. The signal travels after the ionosphere through the troposphere. This layer is the lowest part of the atmosphere which extends from about 20km above sea level until the earth's surface. This layer can also delay the satellite signal, this is mainly related to the wet and dry conditions within the layer (Karaim et al., 2018).

When the signal is closer to the receiver it is possible that the signal reaches the antenna via more than one path caused by signal reflections from the ground or surrounding structures, for example, buildings. Usually one of the received signals is the direct signal, the other signals are reflected signals. These reflected signals are delayed versions of the direct signal, these signals result in errors when making measurements. The errors caused by this effect are referred to as Multipath errors (Georgiadou and Kleusberg, 1988; Karaim et al., 2018).

2.3.3 System errors

There are also errors which are a result of the system itself, for example, satellite orbit errors and receiver noise. The location of the receiver is determined by the distance between the satellite sending the signal and the receiver. However, for this it is important to know the location of the satellite. The orbit of the satellite is estimated by mathematical models; however, this is subject to errors when comparing it to reality. It is possible to reduce these errors when there are global or local network corrections available (Karaim et al., 2018).

Another possible source of error is the geometry of the satellites used when determining your position. An even spread of satellites in the sky will result in more accurate position determination than when the satellites are more clustered together. There are several dilution of precision (DOP) indicators which describe the error caused by the relative positions of GNSS satellites. The PDOP represents the Position Dilution of Precision, the HDOP represents the Horizontal Dilution of Precision, and the VDOP the Vertical Dilution of Precision. A smaller DOP number indicates a better geometry and therefore less possible error in the accuracy of the location position (Langley, 1999; ESRI, 2020). A higher number of satellites can improve the satellite geometry; however, it is not a guaranty.

There are also error sources at the receiver end, referred to as receiver noise. It is considered white noise and it can be minimised however it cannot be completely prevented. There is a variety of noise types which comprise receiver noise. Thermal noise and noise by system components like the antenna and cables are examples of noise types (Karaim et al., 2018; Langley, 1997).

2.4 GNSS height determination

The GNSS technology has many positive aspects, however, a weakness of the system is that the initially indicated heights are not physically meaningful. The height provided by the GNSS is the height relative to the ellipsoid. This ellipsoidal height is a mathematical simplified representation of the shape of the earth (Fotopoulos, 2003; Brown et al., 2011). It is not a relative height to a reference surface; this reference surface is for instance in the Netherlands the Normaal Amsterdams Peil (NAP). This

referenced height is also referred to as orthometric height. The difference between the ellipsoidal height and the orthometric height is referred to as the geoid height. How these different heights relate to each other can be seen in Figure 5. Here it is also visible that the orthometric height is calculated by subtracting the geoid height from the ellipsoidal height.

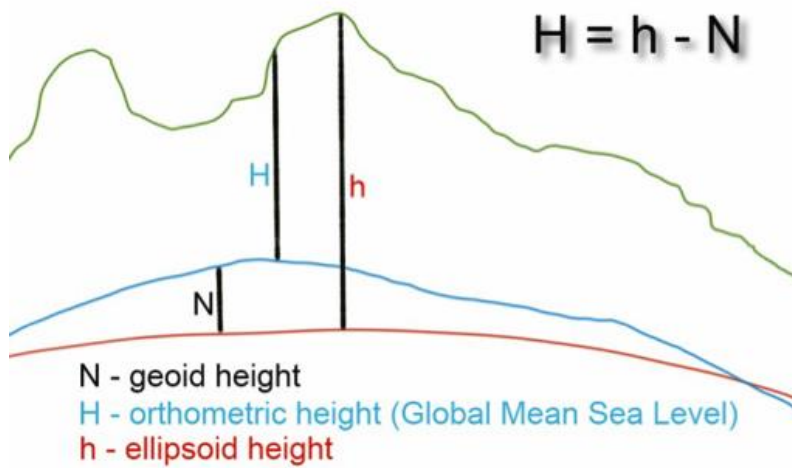


Figure 5 A schematic overview of the geoid height (N), the orthometric height (H) and the ellipsoidal height (h). Source: unavco, 2020

The geoid height can be obtained from a regional gravimetric geoid model or a global geopotential model (Fotopoulos, 2003). A widely used global geopotential model is the EGN96 model (Lemoine et al., 1998). This model is also the default model the ArduSimple RTK setup. Besides global geopotential models there are also regional gravimetric models. These models can provide a higher level of detail and more accurate data (Fotopoulos, 2003).

3 Methodology

This chapter is divided in two main blocks. The first block will focus on quality assessment for the MAPIR Survey 3 sensor data and the second block on the ArduSimple RTK System.

3.1 MAPIR

As mentioned before the NDVI values of the MAPIR Survey 3 sensor data are unrealistically low, which affects the usability of the data. Firstly, a quality assessment was carried out in order to assess the reasons behind the unrealistically low NDVI values. Secondly, the MAPIR data was compared to satellite data. This was done to assess if based on correlations between the MAPIR bands and the satellite data bands it could be possible to develop a correction factor for the MAPIR data, which would enable to generate usable NDVI values

3.1.1 Raw vs. calibrated data

The raw data of the MAPIR sensor needs to be pre-processed before it can be used for the NDVI calculations. One of the pre-processing steps is to calibrate the data based on a calibration ground target using the empirical line method. The ground target contains four compartments, the reflectance values of each of the compartments have been measured by a spectrometer. Within the calibration process, the captured reflectance values are compared to the known reflectance values of the ground target compartments. This is done in MAPIR software (MAPIR, 2020b). After the images are calibrated, they are combined to form an orthophoto mosaic. Agisoft Photoscan was used for this.

Reflectance histograms were created for both the uncorrected and corrected orthophoto mosaics of the MAPIR Survey 3 data. This was done for multiple locations. Reflectance histograms were made for the entire location and for selected homogeneous vegetated areas within the locations. The comparison of the reflectance histograms was done to show if and how the response of the bands changed during the calibration. Three locations were analysed: Belmermeer (the Netherlands), Nhamatanda (Mozambique), and Westmorland (the United States). The data from Westmorland is made available by MAPIR, as an example dataset (MAPIR, 2020c). The NDVI calculations based on this MAPIR example data are realistic. The other datasets are from FutureWater. It is of interest if there is a difference in reflection pattern and in the response on the calibration process between the MAPIR data and FutureWater images.

Multiple flights were made on the same location in Belmermeer in the Netherlands on 29-05-2019, the second (F02) and the third (F03) flights were used for the analysis. This Belmermeer location is characterized by healthy grassland. The data from Nhamatanda, Mozambique contains multiple fields with varying vegetation. Two plots were selected, one with CROP1 and the other with CROP2. The flight was made on 04-12-2019. Rapini is the dominant crop depicted in the data of Westmorland in the United States. This data was from 01-11-2018. The areas which were analysed are shown in Annex I.

The image quality assessment after radiometric correction is often analyzed with the relative values of mean errors (R-RMSE) (Wierzbicki et al., 2018). This indicator was also used in this case. The R-RMSE is expressed as a percentage, where low percentages indicate a better preservation of the spectral information (Wierzbicki et al., 2018; Cakir and Khorram, 2008). The R-RMSE is determined by the following formula (Wierzbicki et al., 2018):

$$R - RMSE_k = \sqrt{\frac{\sum_{i=1}^N \left(\frac{DN_{f \text{ used } (k),i} - DN_{original (k),i}}{DN_{original (k)}} \right)^2}{N}}$$

Where DN is the pixel value, i is the pixel number in band k , k is the number of the spectral band, and N is the number of observations. This analysis has done for the selected homogeneous vegetated areas within the locations. The area of this selection was reduced for the images of both the Dutch flights and for the side in the USA. This was done to reduce the computational time.

3.1.2 Satellite comparison

Satellite data is widely used for NDVI calculations. The red and near-infrared (NIR) bands of the satellite data are used for the generation of the NDVI. The MAPIR sensor has an OCN filter and uses the Orange and NIR bands for the NDVI calculations. The hypothesis is that there are correlations between the NIR bands of the MAPIR and satellite data and between the Orange and Red bands of the two sources. It is assessed if based on these correlations it could be possible to develop a correction factor for the MAPIR data which would enable to generate usable NDVI values.

Two locations were selected for this analysis; an agricultural area with Rapini in Westmorland in The United States and an agricultural grassland area in Belmermeer in The Netherlands. The data from Westmorland was made available by MAPIR, as an example dataset (MAPIR, 2020c). For the location in Belmermeer, there were two flights available of the same location. Both flights were analysed.

The satellite data of Sentinel-2A and Landsat 8 was used. The Sentinel-2A data was used for the analysis with the two flights from Belmermeer and the Landsat 8 data was used for the flight of Westmorland. Initially, the aim was to use Sentinel-2A for both locations, however, there was no appropriate Sentinel-2A data available for the location in Westmoreland for the same period the UAV flight was made. The MAPIR UAV data of Westmorland was from 01-11-2018 and the Landsat 8 data to which it was compared from 05-11-2018. Both the UAV flights of Belmermeer were from 29-05-2019, the Sentinel-2A data was from 18-05-2019.

The Sentinel-2A and Landsat 8 data was accessed through Google Earth Engine (GEE). GEE is a cloud-based platform which enables users to access and process satellite images and geospatial data (Google, 2020)

The Sentinel-2A data has a spatial resolution of 10m for the Red and NIR bands (ESA, 2020) and the Landsat 8 data has a resolution of 30m (NASA, 2020). The MAPIR data was resampled with the bilinear method to match the resolution of the Sentinel-2A data or the Landsat data in order to compare the two sources. A linear regression analysis was performed in R to find the correlation between the NIR bands of the two sources and the correlation of the MAPIR Orange and Sentinel Red band.

3.2 The ArduSimple RTK System

The ArduSimple RTK system consists of two 'simpleRTK2B' boards. One of these boards functions as the base station and the other one is the rover station. The schematic setup of the base station and the rover can be seen in Figure 6. Both the base station and the rover are connected to a U-blox GNSS Multiband antenna and are powered by the 'Power+GPS' port. The base station is equipped with a WiFi NTRIP Master, this enables a WiFi communication link between the base station and the rover. On the rover station the 'TX' and 'RX' ports are connected, to enable the correct messages. The configuration of the boards was done with U-Blox software U-center 19.12. Annex IV contains the user manual of the ArduSimple RTK system. To test the performance of the system three main experiments were conducted, which will be described below.

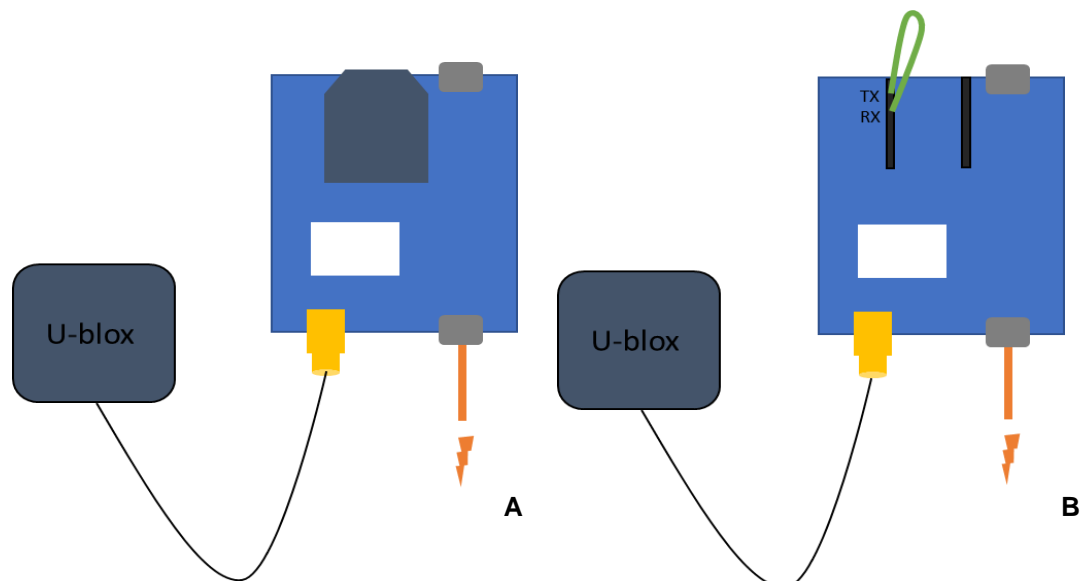


Figure 6 The schematic setup of the base station (A), and the rover station (B)

3.2.1 Test 1

This test was done to test the performance of the ArduSimple rover in an RTK setup compared to an established RTK system. The ArduSimple rover was connected to an NRTIP connection to a base station located in Radio Kootwijk: KOS100NLD0. This base station is one of the multiple base stations TU Delft has set up in the Netherlands (<http://gnss1.tudelft.nl/dpga/>). The station in Radio Kootwijk was selected due to its closest proximity.

The established RTK system which was used for this was the Topcon Hiper V. This system has 2 cm accuracy. The rover of the Topcon connects to base stations of 06-GPS RTK network (06-gps, 2020).

The test was conducted on the Wageningen University campus. The U-shaped hill located next to the Orion building (Fig. 7) was sampled with 11 transects, with five points each. The points were clearly marked to ensure that both systems would sample the same locations. The 55 points were sampled with both the ArduSimple and the Topcon RTK system. The latitude, longitude and altitude of all points were recorded. The difference between the measured points of both systems was compared in X, Y, and Z direction. Furthermore, the line distances between the corresponding points were calculated.



Figure 7 The sampled locations on the U-shaped hill at the Wageningen University campus

3.2.2 Test 2

The second test was focused on the base station. The aim of this test was to discover the required time the base station needs to determine an accurate location. The user of the ArduSimple RTK system has two options to initialise the base station. The first option is to provide the base station with a known surveyed location, this is preferred since this will give a more accurate result. The second option is to let the base station determine its own location, where after a certain time the location will be fixed and the sending of the correction messages will start. This option is referred to as the 'Survey-in mode'. The base station was placed under clear sky conditions. The location (latitude, longitude and altitude) of the station was recorded after 2, 5, 10, 20, 30, 60, 90, 120, 150, 180, 210, 240, 270, 300, 330, 360, 390, and 420 minutes. The location of the base station was also determined by the rover station with an RTK connection with the KOS100NLD0 base station. This was used as the reference location to which the locations of the ArduSimple base station were compared. Besides the location comparison, the PDOP, HDOP and VDOP were also determined for each measurement.

3.2.3 Test 3

Within this test the overall performance of the combined, rover and base station, ArduSimple RTK system was assessed with a focus on the settings within the base station. There were four sets of data points collected under different settings (Table 1):

- For the first set of points, the base station was set to the 'survey-in' mode, where the base station had 10 minutes to determine its position with an accuracy of a minimal of 2 meters before the location was locked and the rover was connected.
- The second set of points were taken when the base station was provided with a known surveyed location, where the altitude was set to the ellipsoid height.

- For the third set, the location of the base station was also provided, this is also referred to as fixed mode. The altitude provided in this set was the 'Normaal Amsterdams Peil' (NAP) height.
- The fourth set of points were taken when the rover was connected to the previously mentioned base station in Radio Kootwijk; KOS100NLD1.

Table 1 An overview of the settings during the different sets of measurements.

Name of set	Base station location mode	Provide Altitude	Rover connected to
'SURVEY-IN'	Survey-in	-	Own base station
'Own_Base_ELL'	Fixed	Ellipsoid	Own base station
'Own_Base_NAP'	Fixed	NAP	Own base station
'Base_KOS'	-	-	KOS100NLD1

The base station was in each set placed on the same location, namely on a 'Rijksdriehoekstelsel' (RD) point at the 'Ginkelse hei' near the town of Ede (NSGI, 2020; Rijkswaterstaat, 2020). This location (Fig. 8) was selected because it was in a clear sky environment, clearly marked with a concrete pillar with an iron rod in the centre to indicate the exact location, and relatively close to the office of FutureWater. In addition, this RD-point was on top of a hill which was also interesting from an elevation measurement point of view. The location of the point is Lat: 52° 02' 40,44912", Lon: 5° 42' 22,22006", and an altitude of 47.839m NAP. To attain the ellipsoid height for this point, the Dutch NLGEO2004 geoid model was used (Crombaghs and de Bruijne, 2004). The sampled points were compared in X, Y, and Z direction and also the line distance between the measured points was determined. The elevation was corrected to have all the same format, be able to compare the sampled points in the Z direction.

Each set consists of 24 points taken on the same locations. The four corners of the concrete pillar were sampled. In the extension of each corner of the pillar, there were four points, with 2.5 to 3 meters between the points. There were four additional points, each at a different side of the pillar at a distance of 10m. The difference between the measured points of the four sets was compared in X, Y, and Z direction. The line distances between the corresponding points were also calculated.

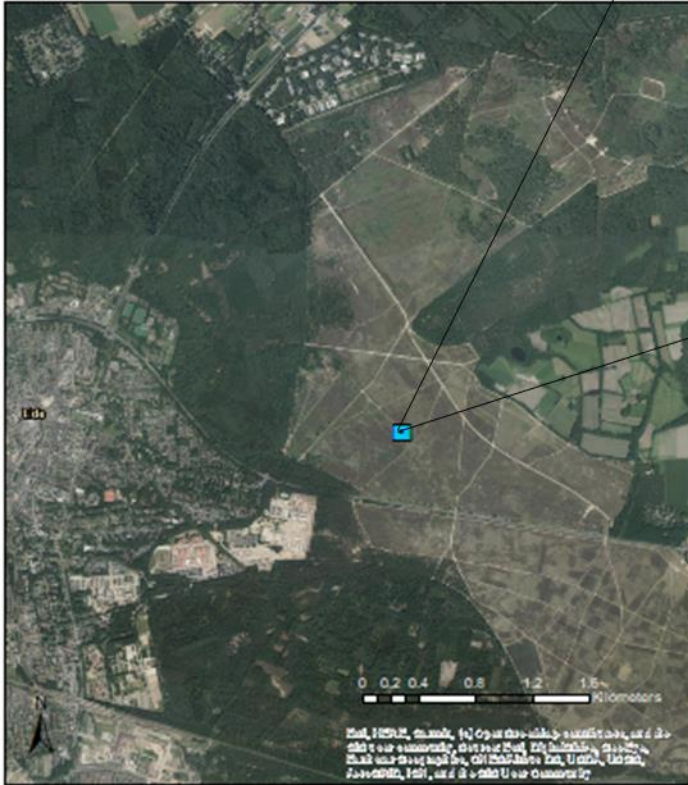


Figure 8 The location of the RD-point on the 'Ginkelse hei' near the town of Ede.

4 Results and discussion

4.1 MAPIR image analysis

In this chapter, the results of the MAPIR image analysis will be presented. The first subchapter will give the results of the created reflectance histograms. The second chapter will provide the results of the comparison with satellite data. The discussion of the provided results in this chapter will directly follow the given results. The last chapter will address general discussion points.

4.1.1 Reflective histograms

Within this subchapter the reflectance histograms of the selected homogeneous vegetated areas will be provided, this will be of the raw and the calibrated images. The reflectance histogram of the overall images can be found in Annex II. As mentioned in the introduction, the MAPIR Survey 3 sensor has an OCN (Orange/Cyan/Near-infrared) filter. Band 1 is orange at 615nm, cyan at 490nm is Band 2 and Band 3 is the near-infrared band at 808nm.

The reflectance histograms of MAPIR's example data, both the raw and processed data, are shown in Figure 9 and 10. The Orange and Cyan bands have a similar pattern in the unprocessed image and the NIR band has a peak of the same height, however with higher data values. When comparing the histograms of the unprocessed and the calibrated images, it shows the effect of the calibration. Within the calibration process, the peaks of the Orange and Cyan bands became narrower and shifted to the left. This was the result of more concentrated and lower data values.

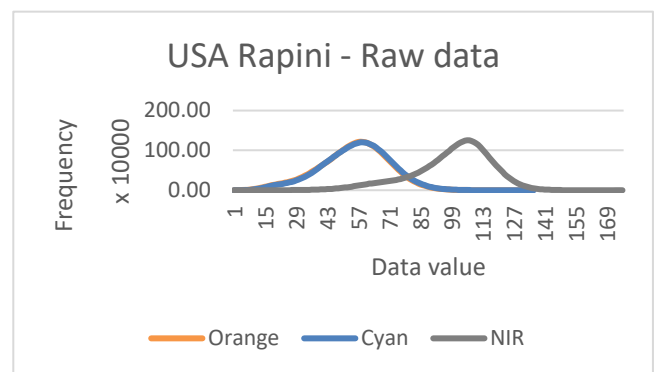


Figure 9 The reflectance histogram of the raw image with the land use of Rapini in the USA

Figure 11 depicts the reflection histogram of the raw data of F02 in Belmermeer, the Netherlands. All bands show comparable patterns. However, the Cyan and NIR bands show the most similarities. When looking at the calibrated image (Fig. 12) it can be seen that the Cyan and NIR bands have a less similar pattern, however, the difference between the bands is still very limited. This similar pattern in the calibrated image also explains the low NDVI values. The values of the Orange and NIR bands, which are used for the NDVI calculations, are generally close together. When going back to the unprocessed data it is also striking that the difference between the Orange and NIR bands is so small. It is healthy green vegetation, therefore it was expected that there would already be a large difference between the Orange and NIR bands, because it would have reflected a large portion of the near-infrared and absorbed most of the visible light (Weier and Herring, 2020).

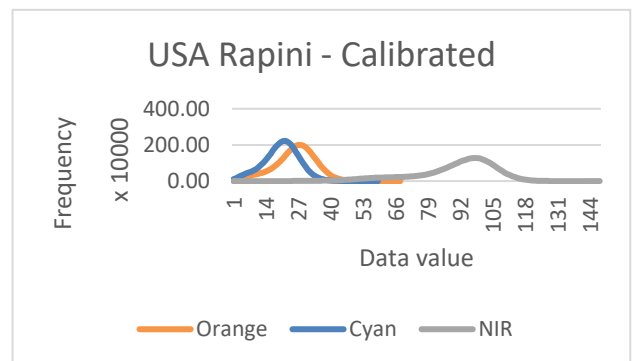


Figure 10 The reflectance histogram of the processed image with the land use of Rapini in the USA

The same reflectance response is visible in the other flight which was conducted in Belmermeer (Fig 13 and 14). The bands also show here comparable reflectance response with little deviation between the bands. This is the case for both the non-calibrated and calibrated image.

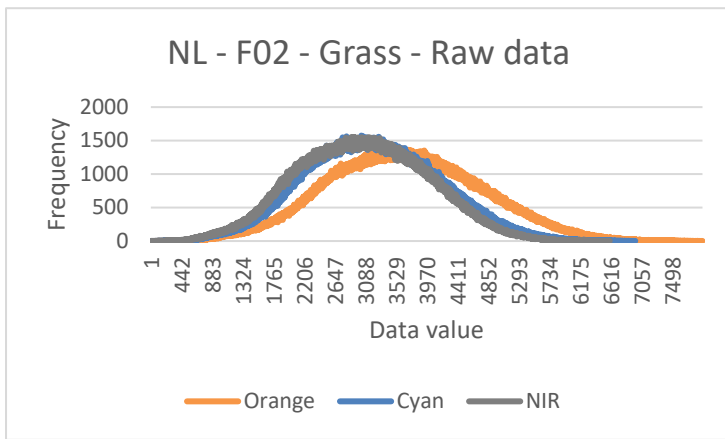


Figure 11 The reflectance histogram of the land use grass of the raw image of F02 in Belmermeer, NL.

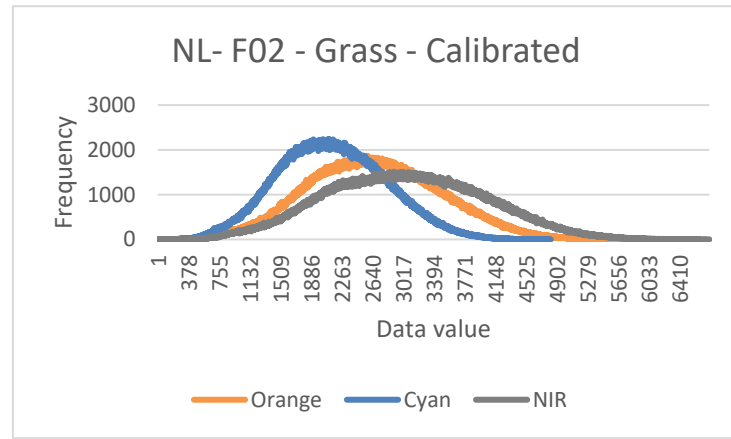


Figure 12 The reflectance histogram of the land use grass of the calibrated image of F02 in Belmermeer, NL.

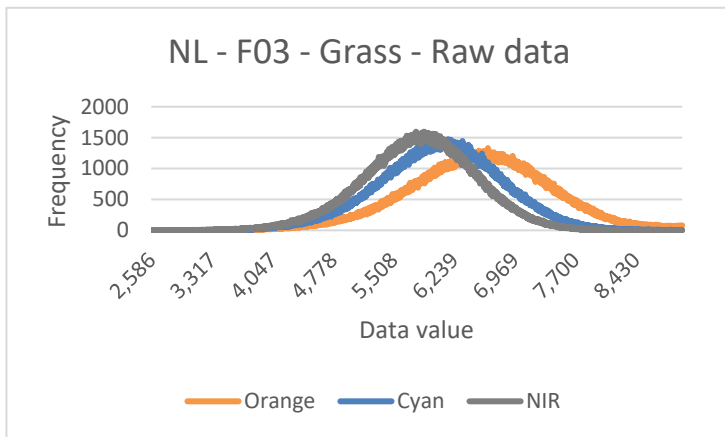


Figure 13 The reflectance histogram of the land use grass of the raw image of F03 in Belmermeer, NL.

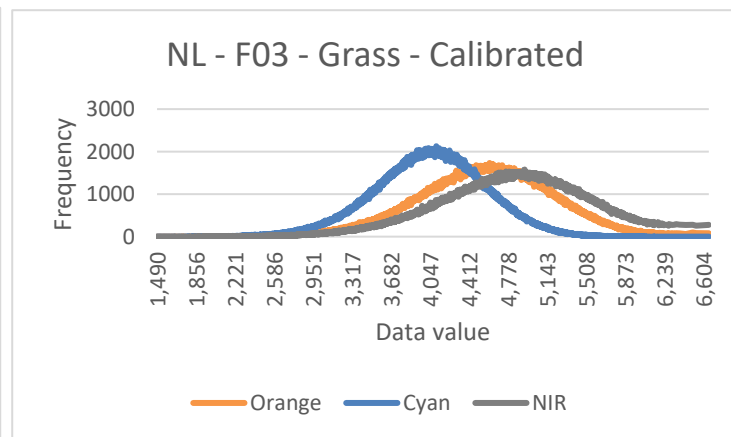


Figure 14 The reflectance histogram of the land use grass of the calibrated image of F03 in Belmermeer, NL.

Figure 15 and 16 show the reflectance response of the raw and calibrated image of the field with crop 1 in Mozambique and Figure 17 and 18 for the crop 2 field. It can be seen that the Orange and NIR band show a vary comparable response in both the raw images (Figure 15 and 17). The Orange and NIR bands were less similar for crop 1 in the calibrated image, however, for crop 2 the band maintained their similar response.

The little difference in response of the Orange and NIR bands in the raw image as well as in the calibrated image was not as expected. Both the fields were with healthy vegetation, it was expected to have low reflection in the visible and high in the infrared, which would have caused a non-corresponding response of the Orange and NIR bands.

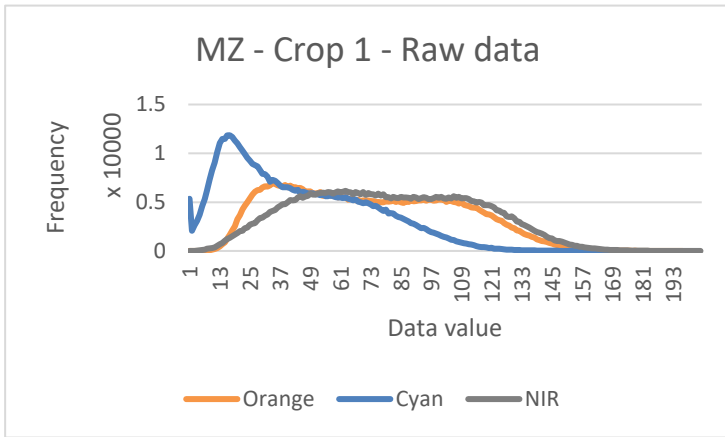


Figure 15 The reflectance histogram of the land use Crop 1 of the raw image of Mozambique

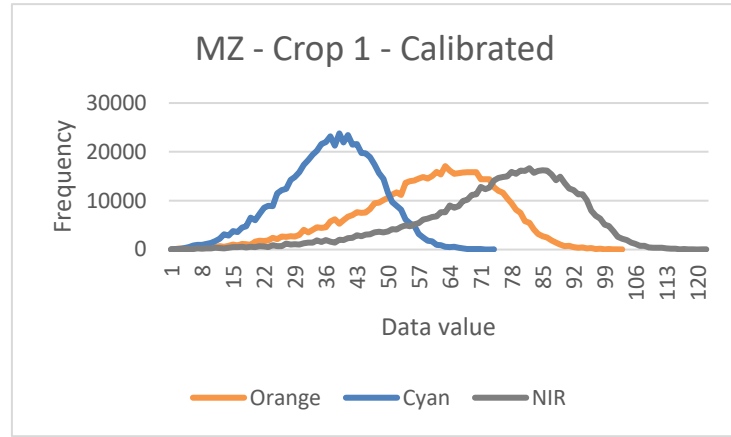


Figure 16 The reflectance histogram of the land use Crop 1 of the calibrated image of Mozambique

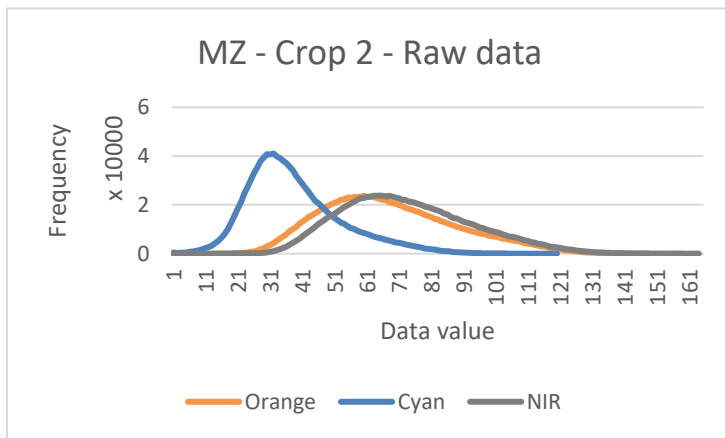


Figure 17 The reflectance histogram of the land use Crop 2 of the raw image of Mozambique

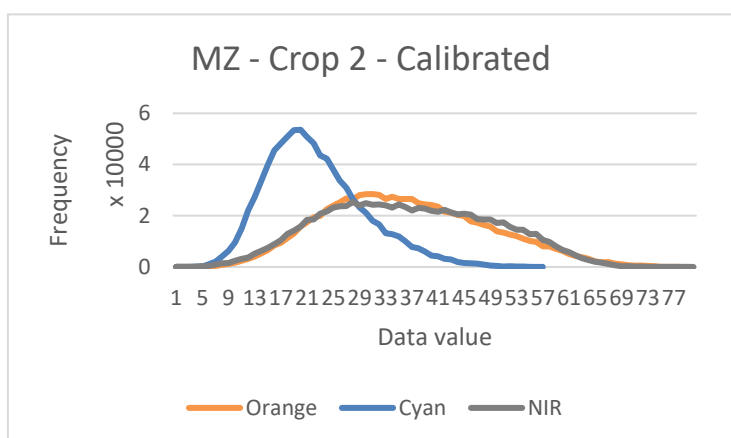


Figure 18 The reflectance histogram of the land use Crop 2 of the calibrated image of Mozambique

Table 2 gives the R-RMSE in percentages for each band of the selected areas. In this table, it can be seen how each band changed as a result of the calibration process. This accounted both for over and underestimation. Band 3, which is the NIR band, changed the least compared to the other bands. Which means that the calibrated pixel values are relatively closest to their original observed pixel values (Cakir and Khorram, 2008). However, there are some variations between the locations. Some variations were expected since the calibration corrects for local reflectance conditions (e.g. due to cloudiness, time of day) during the moment of when the image was captured. However, overall all the R-RMSE values are relatively high when comparing it to literature (Aiazzi et al., 2002; Cakir and Khorram, 2008; Wierzbicki et al., 2018). Indicating that the calibration process altered the images relatively much. This is the case for both the MAPIR example data as for Future Water's data, which adds to the assumption that the raw images of FutureWater's MAPIR sensor did not give a correct initial response.

The images of the MAPIR sensor of FutureWater all showed an unexpected response. The Orange and NIR bands gave a very similar reflection response in the raw images. This did not sufficiently improve after calibration. The similar response was not expected due to the healthy vegetation types depicted in the images. The similar response for the Orange and NIR band explained the unrealistically low NDVI values. The example data of MAPIR gave the expected response for the depicted vegetation, namely a lower reflection in the orange band and higher in the NIR band. This difference between the Orange and NIR band got more defined after calibration.

Table 2 The R-RMSE (in %) for each band of the selected areas for each location.

Location	Orange band	Cyan band	NIR band
USA	60.78	64.73	21.00
MZ_CROP1	58.92	325.27	41.07
MZ_CROP2	36.98	99.33	31.58
NI_F02	44.95	58.10	11.63
NI_F03	49.73	61.48	17.78

4.1.2 Comparison with satellite data

A comparison between the bands which are used for the NDVI calculations of the MAPIR sensor and satellite data has been done to discover if and how the MAPIR data can be corrected based on satellite data in order to get workable NDVI values.

In Figure 19 the comparison between band 1 (orange) of the MAPIR sensor and band 4 (red) of Landsat 8 is shown for the location in the USA. It can be seen that there is no correlation between the two sources. When looking at Figure 20, which shows the correlation between the NIR bands of the MAPIR sensor and Landsat 8, it becomes clear that there is a correlation between the two sources, namely an R^2 of 0.769. Figure 21 and 22 give the correlations between the bands used for the NDIV calculations of the MAPIR sensor and Sentinel-2 for flight F02 the location in the Netherlands. Here it there is also no correlation between orange and red bands (band 1 of the MAPIR sensor and band 4 for Sentinel-2). The R^2 value for the comparison of the NIR bands is higher, but not high enough for a good correlation. Figure 23 and 24 give the correlations between the bands used for the NDIV calculations of the MAPIR sensor and Sentinel-2 for flight F03 the location in the Netherlands. These figures show the same trend as the figures of F02. There is an R^2 of 0.07 for the orange/red band comparison and an R^2 of 0.27 for the NIR bands.

The resampling could have had an influence on the R^2 value therefore it was not expected to find perfect correlations values, however, it was expected to find some correlation. This eliminates the opportunity to create an accurate correction factor for FutureWater’s MAPIR sensor based on satellite data.

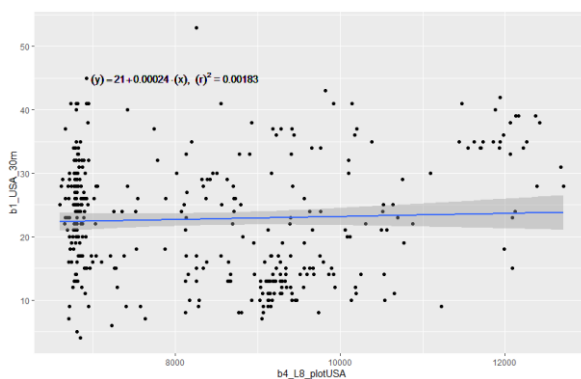


Figure 19 The correlation between Band 1 (Orange) of the MAPIR sensor and band 4 (Red) of Landsat 8 for the entire image of Westmorland, USA

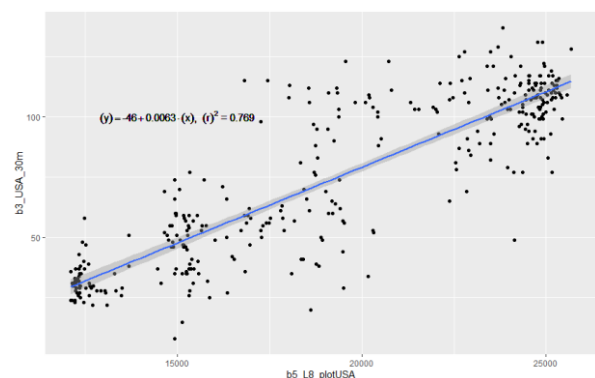


Figure 20 The correlation between Band 3 of the MAPIR sensor and band 5 of Landsat 8 (the NIR bands) for the entire image of Westmorland, USA

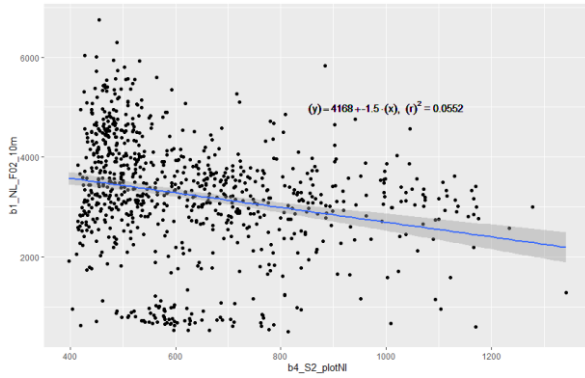


Figure 21 The correlation between Band 1 (Orange) of the MAPIR sensor and band 4 (Red) of Sentinel 2 for image F02 of Belmermeer, NL

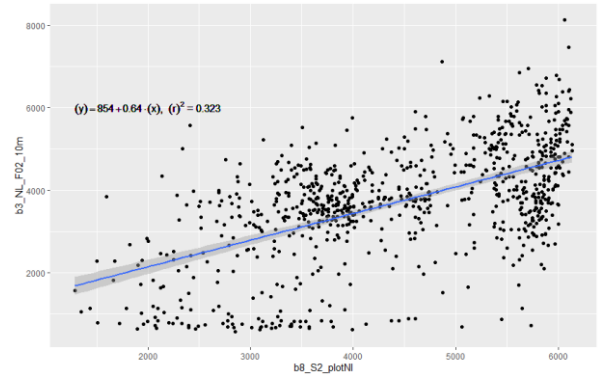


Figure 22 The correlation between Band 3 of the MAPIR sensor and band 8 of Sentinel 2 (the NIR bands) for image F02 of Belmermeer, NL

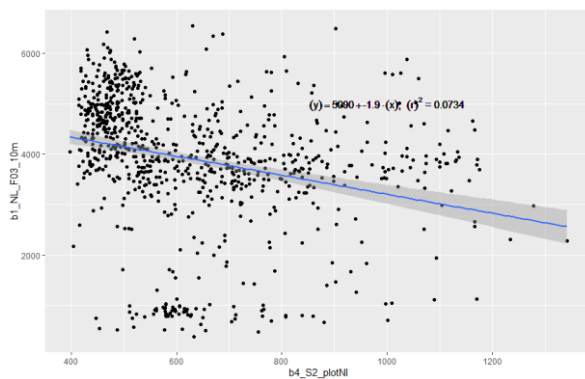


Figure 23 The correlation between Band 1 (Orange) of the MAPIR sensor and band 4 (Red) of Sentinel 2 for image F03 of Belmermeer, NL

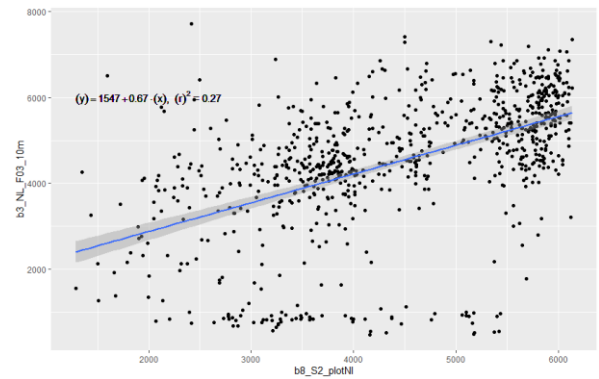


Figure 24 The correlation between Band 3 of the MAPIR sensor and band 8 of Sentinel 2 (the NIR bands) for image F03 of Belmermeer, NL

4.1.3 General performance

FutureWater has multiple MAPIR Survey 3 sensors, which all operate with the same default settings which are recommended by MAPIR. This eliminates the possibility that the unrealistically low NDVI values originate from incorrect settings. It also confirms that it is not an error within just one of the sensors.

Even though the MAPIR sensor data does not provide satisfactory NDVI values it can still provide other functions. It is a sensor which creates images with a very high resolution. This makes it possible to perform visual interpretations. For instance, to visually identify areas where crops experience stress or to determine the land use type.

4.2 The ArduSimple RTK system

The results of the tests which were performed with the ArduSimple RTK system will be provided and discussed per test. The order will correspond with tests described in the methodology.

4.2.1 Test 1

Results

This test was carried out on the Wageningen University campus. The sampling points can be seen in Figure 7. The points were sampled with the Topcon V rover connected to the 06-GPS network and were sampled with the ArduSimple rover which was connected to the KOS100NLD1 base station. 55 points were sampled on the U-shaped hill. The difference between the measured locations by the ArduSimple system has been compared to the measured locations of the Topcon V system. The result of this comparison can be seen in Table 3. This table gives information on the entire set of points, for the comparison per point see Annex III.

The comparison of the measurements of the two systems on the U-shaped hill (Table 3) shows that the differences are in the magnitude of a couple of centimetres. The average difference in the Z-direction is higher than in the X and Y direction. Also, the highest maximum difference between the systems is in the elevation, namely a 10.7-centimetre difference at one sampled point.

Table 3 The comparison between the measurement differences on the U-Shaped hill of the ArduSimple RTK and the Topcon V RTK system.

	<u>U-shaped hill</u>			
	Line distance	ΔX	ΔY	ΔZ
Average (m)	0.030	0.011	0.026	0.060
Min (m)	0.004	0.000	0.000	0.022
Max (m)	0.067	0.044	0.060	0.107
STD (m)	0.014	0.010	0.013	0.018

Discussion

The measured locations on the U-shape hill differ on average 1.1 cm in X-direction, 2.6 cm in Y-direction and 6 cm in elevation. However, these values could have been affected by measuring errors of both systems and the difference in the setup of the systems. Measuring errors could have occurred with both systems by not placing the antennas on the exact same locations. The locations were clearly marked, however when placing the antennas, there is a possibility that they were placed a few mm-cm off the marked location. The antenna of the Topcon was situated on a two-meter-high pole which needed to be manually levelled for correct measurements. In the case that the setup was not completely levelled the antenna of the Topcon would not have been exactly on the marked location. The antenna of the ArduSimple was placed directly on the ground. Another element which influences the quality of the measurements is the used base station. The systems were both using a different base station. This could have had some influence on the compared measurements.

The measurements differed the most in the elevation measurements. This could have been the result of the used geoid height. The Topcon with the 06-GPS RTK network connection applied the geoid height of nlgeo2004 geoid model. Only the orthometric height was available for these measurements. For the ArduSimple RTK both the orthometric and the ellipsoidal height were available, the orthometric height was determined with the EGM96. However, to be able to better compare the measured elevation values, the orthometric height of the ArduSimple RTK was also calculated based on the nlgeo2004 geoid model.

The comparison between ellipsoidal height would have given a more precise evaluation of the performance of both systems.

However, even when not taking the possible measuring errors into account, both systems gave very comparable output in the X and Y direction. This indicates that the ArduSimple RTK can compete with established RTK systems which promise cm accuracy. However, it needs to be noted that the ArduSimple RTK system required more time to attain a fixed position each time the antenna was moved.

4.2.2 Test 2

Results

The second test was done to evaluate the 'Survey-in mode' of the base station. Figure 25 shows the shift in the location of the base station through time. The black square indicates an RTK measured point. This point was used as a reference point to which the base station locations were compared. Table 4 gives an overview of the difference between the measured RTK point and the locations of the base station over time. In addition, it is indicated how many satellites were in view, the PDOP, HDOP, and VDOP. The DOP indicators were all between 0-2 which indicated an excellent geometry. In general, the base station's location became more accurate through time. However, the difference in Y direction was relatively lower during the beginning of the experiment compared to halfway (90-270 minutes) and also, even though to a lesser extent, compared to the end of the experiment (>300 minutes).

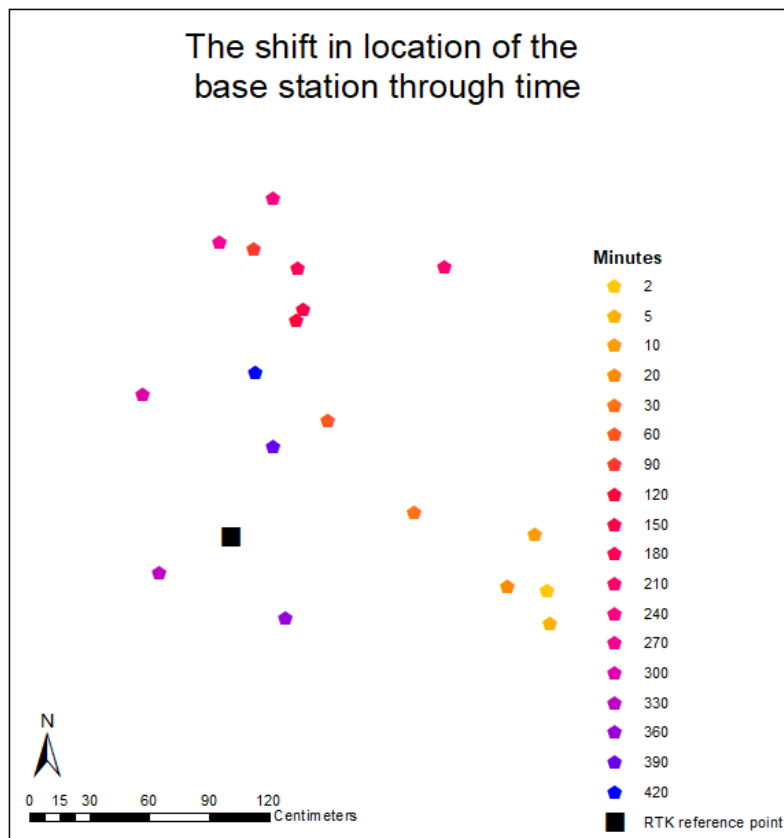


Figure 25 The shift in location of the base station through time

Table 4 Result test 2, time measurements

Minutes	Line Distance	ΔX	ΔY	ΔZ	Number of satellites	PDOP	HDOP	VDOP
2	1.602	1.579	0.269	3.647	22	1.4	0.8	1.15
5	1.649	1.591	0.436	3.747	23	1.2	0.7	0.97
10	1.520	1.520	0.009	4.547	28	1.2	0.6	1.04
20	1.407	1.384	0.252	4.047	29	1	0.6	0.8
30	0.921	0.913	0.118	4.047	29	1.1	0.6	0.92
60	0.757	0.487	0.579	1.547	34	1.1	0.6	0.92
90	1.436	0.117	1.431	1.747	31	1.1	0.7	0.85
120	1.127	0.325	1.079	1.047	30	1	0.6	0.8
150	1.191	0.359	1.135	0.053	35	1	0.5	0.87
180	1.381	0.336	1.340	0.853	36	1	0.5	0.87
210	1.716	1.068	1.343	1.253	36	1	0.5	0.87
240	1.704	0.208	1.691	1.847	38	0.9	0.5	0.75
270	1.468	0.055	1.467	2.147	37	1	0.5	0.87
300	0.833	0.442	0.706	3.147	36	1	0.5	0.87
330	0.402	0.358	0.184	2.847	35	1	0.5	0.87
360	0.488	0.274	0.404	1.147	37	0.9	0.5	0.75
390	0.497	0.213	0.449	0.347	33	0.9	0.5	0.75
420	0.828	0.120	0.819	0.247	35	0.9	0.5	0.75

Discussion

In general, the location determination became more accurate over time. However, the location accuracy was better at 330 and 360 minutes than at 420 minutes. It would have been interesting to see the effect of even a longer experiment duration, however, due to weather conditions this was not possible.

However, the offset was still relatively large after 7 hours. This is also the offset by which the rover station will do its measurements when it is connected to the base station. The precision of the rover measurements will be good; however, the measurements will have an offset. This is an element which needs to be considered. More on the use of the 'Survey-in mode' of the base station in the coming chapter.

4.2.3 Test 3

Results

Within this experiment the overall performance of the combined, rover and base station, ArduSimple RTK system was assessed with a focus on the settings within the base station. There were four sets of data points collected under different settings. The setting can be found in the methodology, under section 1.3.1.3 Test 3. Figure 26 shows the output of the measurements with the different settings. Especially the 'SURVEY-IN' set varies relatively much from the other sets. The measurements of the other three sets are relatively close to each other. A more detailed comparison between the measurements of the sets will be given in the remainder of this chapter. Table 5 gives an overview of the compared sets; the indicated numbers of the comparisons will also be used in the following tables in this chapter. The sets are all compared to the 'Base_KOS' set. The settings used for this set were the same as in 4.2.1 Test 1. The other sets are compared to this set since it is known how the ArduSimple with the 'Base_KOS' settings compares to an established RTK.

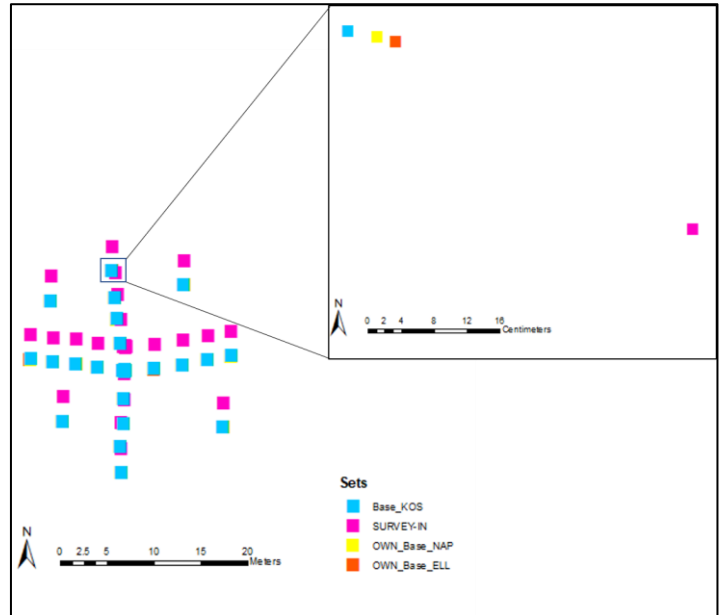


Table 5 An overview of the compared sets.

Set which are compared	
Base_KOS	SURVEY-IN
Base_KOS	Own_Base_ELL
Base_KOS	Own_Base_NAP

Figure 26 The outcome of the measurements of the sets with different settings.

Tables 6 until 9 give information regarding the combined points per compared set, information per point can be found in Annex III.

When looking at Table 6, it can be seen that the average line distance of the comparison with the SURVEY-IN mode is relatively high with 2.6 meters, where the other two comparisons have an average line distance of a couple of centimetres. However, the standard deviations of all the comparisons are in the same order. This indicates that the line distances between the points of the compared sets are generally in the same range.

When comparing Table 7 and 8 it becomes clear that the large deviation from the SURVEY-IN comparison is mainly the result of an offset in the Y direction. The average variation in X and Y direction for the other comparisons are in the order of a couple of centimetres.

The difference in average elevation (Table 9) is largest for the SURVEY-IN comparison. The difference in average elevation for the other two comparisons are relatively the same.

Table 6 Line distance information of the compared to sets

	Line Distance		
	SURVEY-IN	Own_Base_ELL	Own_Base_NAP
Average	2.606	0.039	0.031
Max	2.632	0.069	0.054
Min	2.582	0.015	0.011
std	0.011	0.012	0.012

Table 7 The difference in X direction of the compared to sets

	ΔX		
	SURVEY-IN	Own_Base_ELL	Own_Base_NAP
Average	0.098	0.025	0.019
Max	0.123	0.059	0.036
Min	0.038	0.002	0.000
std	0.020	0.012	0.010

Table 8 The difference in Y direction of the compared to sets

	ΔY		
	SURVEY-IN	Own_Base_ELL	Own_Base_NAP
Average	2.604	0.027	0.022
Max	2.630	0.062	0.046
Min	2.580	0.005	0.001
std	0.011	0.012	0.012

Table 9 The difference in Z direction of the compared to sets

	ΔZ		
	SURVEY-IN	Own_Base_ELL	Own_Base_NAP
Average	0.814	0.138	0.125
Max	0.847	0.172	0.153
Min	0.727	0.087	0.092
std	0.023	0.017	0.016

Discussion

When comparing the 'Survey-in' mode measurements with the other sets it can be seen that this set gives the least accurate measurements. However, based on the standard deviations it can also be seen that the offset is relatively consistent when comparing it to the other sets. This indicates that the RTK connection with the own base station in 'Survey-in' mode gives similar precise measurements as the other sets. The determined location of the base station was off in the 'Survey-in' mode, which resulted in an overall shift in the measured location with the rover. However, since the measurements are precise it is possible to correct them when the offset is known or use the measurements directly when the accuracy is not of importance, but the precision is (e.g. the dimensions of a field).

The average difference in X and Y direction was relatively small between the points of the sets which used the own base station (Own_Base_ELL and Own_Base_NAP) and the points of the set which used the base station in Radio Kootwijk (Base_KOS). Even though the differences X and Y-direction were relatively small, the difference in Z-direction is larger. Since the same geoid model was used for all sets, this could not be a result of the difference between geoid models. It could be the result of the provided elevation to the base station. The elevation data was from the year 1998. The selected RD point was the only RD point in the area which was relatively close by and had an elevation value, many RD points were missing this data (NSGI, 2020). It is possible the elevation changed slightly over time. The base station in Radio Kootwijk was setup in 2019 (TU Delft, 2020).

Another reason for the difference between the sets could be the baseline, the distance between the rover and the base station. The baseline used for the 'Own_Base_ELL' and 'Own_Base_NAP' sets was in the order of a few meters, however, the baseline for the set 'Base_KOS' was a bit more than 16km. A longer baseline can lead to less accurate measurements, since the GNSS errors can deviate more between the location of the rover and the base station (Landau et al., 2003; Vollath et al., 2002). Therefore, it is possible that the measurements of the 'Own_Base_ELL' and 'Own_Base_NAP' sets are more accurate than the 'Base_KOS' set and therefore even more comparable to an established RTK system. However, this was not tested.

Comparison 2 and 3 gave similar results. Both the 'Own_Base_ELL' and 'Own_Base_NAP' sets used the same base station. This base station was provided with the same known surveyed location and the same geoid model was used. Therefore, the main reason for the difference between the measurements of the sets is human measurement errors. However, it needs to be noted that the difference is relatively very small; on average nine millimetres in both X and Y direction.

4.2.4 General performance

The ArduSimple RTK system is a very compact system, which makes it easy to transport. All the required elements will easily fit in a hand luggage bag. In addition, the system is operational with the use of a mobile phone or a laptop. These are devices that are usually already available to you on field days and easy to use. The app SW maps is a real added value when working with a mobile phone. This app has an easy to work with interface, which makes it easy to handle. In addition, the app helps to work in a structured manner and provides a clear overview of your data.

An element to take into account is that the time required to get an 'RTK FIX' position (the moment when the RTK position is the most accurate) for each new point was longer with the ArduSimple RTK than with the Topcon. This will result in longer sampling time when working with the ArduSimple RTK. Another downside to the ArduSimple RTK system compared to the more established systems is that the system is quite fragile. The system is not water and dust resistant. A case around the ArduSimple circuit board will help, however, it will still not be possible to work with the system in rainy condition.

When using an own base station in your RTK setup, it is advised to provide the base station with a known surveyed location; use the 'Fixed mode'. This gives accurate and precise measurements. However, when a known surveyed location is absent, it is possible to use the 'Survey in' mode, which determines the location of the base station itself. When opting for this, it needs to be kept in mind that there could be a shift in the measurements due to an inaccurate base station location determination. The measurements are precise. Therefore, when knowing the offset, this can be corrected. An option for this would be to take some measurements on visually outstanding objects. These points can afterwards be linked to areal imagery. When the offset is known because of the few reference points, the other points in your dataset can be corrected with this. Another thing to take into consideration when using the 'Survey in' mode is the duration of the location determination. With a longer duration the accuracy will improve.

However, this requires a constant power source and a secure and dry location for the antenna. This might not always be available when working in the field, therefore some compromises might need to be made.

5 Conclusion

To improve the accuracy and consistency of FutureWater's geodata, two elements have been assessed. The first element consisted of a quality assessment of FutureWater's MAPIR Survey 3 sensor data and to determine the possibility of developing a correction factor based on satellite data. The second element focused on getting the ArduSimple RTK system operational and assessing its performance.

The images of the MAPIR sensor of FutureWater all showed an unexpected response. The Orange and NIR bands gave a very similar reflection response in the raw images. The similar response was not expected due to the healthy vegetation types depicted in the images. Usually, when analysing healthy vegetation, the Orange band should have low values and the NIR high. After the images were calibrated the distribution of the band values did not improve meaningfully. The similar reflectance response for the Orange and NIR band explained the unrealistically low NDVI values. The example data of MAPIR gave the expected response for the depicted vegetation, namely a lower reflection in the orange band and higher in the NIR band. This difference between the Orange and NIR band of MAPIR's example data got more defined after calibration. The calibration process had a comparable effect on the raw data of both FutureWater and MAPIR's data, which adds to the assumption that the raw images of FutureWater's MAPIR sensor did not give a correct initial response.

The possibility to use satellite data to create a correction factor in order to use the MAPIR data for NDVI calculations was assessed. However, it must be concluded that it is not realistic to develop a correction factor for the MAPIR data based on satellite correlations. In all cases, there was no satisfactory correlation between the MAPIR and Sentinel2a bands. Therefore, a correction factor based on satellite data would not give a realistic and satisfactory result.

Once the ArduSimple RTK was operational, the system was assessed on different aspects: the accuracy compared to an established RTK system (the Topcon), the ability of ArduSimple base station to determine its position correctly, and the influence of the used base station.

The ArduSimple reached comparable accuracy in X and Y-direction in comparison to the established RTK system. The measurements of the ArduSimple RTK differed on average 1,1cm in X-direction and 2.6 cm in Y-direction. The average difference in Z-direction was higher, namely 6 cm, however, this could have been affected by the used geoid height.

The ArduSimple base station is able to determine its own location, where the accuracy of this determination will increase with time. When using a base station that has determined its own location it will result in an offset, however, this offset is constant throughout the measurements, which makes it possible to correct for during postprocessing. However, the system will be most accurate when the base station is provided with a known surveyed location.

To conclude:

- FutureWater's data from the MAPIR Survey 3 sensor gave unrealistically low NDVI values. After analysing the data, it became clear that the data did not give the expected initial reflectance response and the calibration did not lead to significant improvements. The Orange and the NIR bands gave very similar reflection responses for the assessed images of FutureWater. These comparable reflection responses of the bands, which are used for the NDVI calculations, are the reason behind the unrealistically low NDVI values. In addition, it was not possible to create a correction factor based on satellite data in order to correct for the MAPIR data.
- The accuracy of the ArduSimple RTK system is comparable to established RTK systems. The system will be most accurate when the base station is provided with a known surveyed location. When there is no known surveyed location available it is possible to let the base station determine its own location, however, this will result in an offset. The measurements will still have the same precision as when the base station was provided with a known surveyed location, which makes it possible to correct for during postprocessing.

6 Recommendations

The following recommendations are given based on the analysis of the MAPIR Survey 3 data:

- The MAPIR Survey 3 might not be the most suitable sensor to use for reliable and consistent NDVI measurements, another sensor would be advised for this.
- The sensor produces very clear and high-resolution images, these images can therefore still be used for other applications. The data can still be used for the detection of vegetation, canopy cover calculations and identification of problem areas within a field.
- It is advised when orienting on a possible new sensor for NDVI calculations, especially when it is a relatively new device, to look whether there is a user platform. This can give information on if and what kind of issues other users encountered. MAPIR has a very transparent website, where it was possible to download unprocessed data and conduct the processing steps with, to experience the workflow and reach the same output. This was a very positive aspect of MAPIR. However, the data of FutureWater gave a different output. Contact with MAPIR did not help. A user platform could in such circumstances help to get informed about other user's experiences.

The recommendations related to the ArduSimple RTK systems are as follows:

- It is advised to use the RTK system with a base station where you provide the base station with a known surveyed location, preferably where the orthometric height is used for the Z value. However, when working with the ArduSimple RTK system on a location where there is not a known measured location, there is the possibility to let the base station determine its location. This will lead to less accurate results, however, the precision is comparable to when the base station is provided with a known surveyed location. Depending on the purpose of the measurements, there is a possibility to correct for the less accurate measurements. If the measurements will be linked to areal imagery there is an option to measure clearly visible or marked objects and link these measurements to these locations in the areal images. It would be enough to do this for a few measurements since the precision of the system is good. If it is known what the offset is of the reference points, it is possible to correct the other points with this offset.
- If there is just a need to know the distance between points, for instance, to measure the area of agricultural plots, there will not be a direct need to correct the measurements.
- A suggestion for further testing with the system would be to test the influence of different baselines (the distance between the rover and the base station). When sampling multiple areas in the same region it would be most convenient to set up a base station on one secure location and leave it on. This location should have a constant power source and a clear sky view, preferably a bit elevated for instance on a rooftop or a balcony. However, in order to do this, it would be good to know if and how the rover's measurement will be affected by a varying baseline.

References

- 06-GPS (2020) Coördinatenstelsel. <https://www.06-gps.nl/coordinatenstelsels/> Last visited: 10-04-2020
- Aiazzi, B., Alparone, L., Baronti, S., & Garzelli, A. (2002). Context-driven fusion of high spatial and spectral resolution images based on oversampled multiresolution analysis. *IEEE Transactions on geoscience and remote sensing*, 40(10), 2300-2312.
- ArduSimple. (2020) <https://www.ardusimple.com> Last visited: 15-01-2020
- Ashby, N. (1995). Relativistic effects in the global positioning system. *Journal of systems engineering and electronics*, 6(4), 199-237.
- Bakuła, M., Oszczak, S., & Pelc-Mieczkowska, R. (2009). Performance of RTK positioning in forest conditions: Case study. *Journal of Surveying Engineering*, 135(3), 125-130.
- Barbedo, J. G. A. (2019). A Review on the Use of Unmanned Aerial Vehicles and Imaging Sensors for Monitoring and Assessing Plant Stresses. *Drones*, 3(2), 40.
- Bidikar, B., Rao, G. S., Ganesh, L., & Kumar, M. S. (2014). Satellite clock error and orbital solution error estimation for precise navigation applications. *Positioning*, 2014.
- Brown, N. J., Featherstone, W. E., Hu, G., & Johnston, G. M. (2011). AUSGeoid09: A more direct and more accurate model for converting ellipsoidal heights to AHD heights. *Journal of Spatial Science*, 56(1), 27-37.
- Cakir, H. I., & Khorram, S. (2008). Pixel level fusion of panchromatic and multispectral images based on correspondence analysis. *Photogrammetric Engineering & Remote Sensing*, 74(2), 183-192.
- Crombaghs, M., & de Bruijne, A. (2004). NLGEO2004-Een nieuw geoidemodel voor Nederland.
- EI-Rabbany, A. (2002). *Introduction to GPS: the global positioning system*. Artech house.
- ESA (2020) Spatial resolution. <https://sentinel.esa.int/web/sentinel/user-guides/sentinel-2-msi/resolutions/spatial> Last visited: 31-03-2020
- ESRI (2020) HDOP. <https://support.esri.com/en/other-resources/gis-dictionary/term/358112bd-b61c-4081-9679-4fca9e3eb926> Last visited: 10-03-2020
- Fotopoulos, G. (2003). An analysis on the optimal combination of geoid, orthometric and ellipsoidal height data (pp. 3914-3914). University of Calgary, Department of Geomatics Engineering.
- FutureWater (2020). TWIGA: Transforming Weather Water data into value-added Information services for sustainable Growth in Africa. <https://www.futurewater.eu/projects/twiga/> Last visited: 14-01-2020
- Georgiadou, Y., & Kleusberg, A. (1988). On carrier signal multipath effects in relative GPS positioning. *Manuscripta geodaetica*, 13(3), 172-179.
- Google (2020) Meet Earth Engine. <https://earthengine.google.com/> Last visited: 27-02-2020

IPCC. (2007) Climate Change 2007: Impacts, Adaptation and Vulnerability. Contribution of Working Group II to the Fourth Assessment Report of the Intergovernmental Panel on Climate

Jackson, R. D., & Huete, A. R. (1991). Interpreting vegetation indices. Preventive veterinary medicine, 11(3-4), 185-200.

Kaplan, E., & Hegarty, C. (2005). Understanding GPS: principles and applications. Artech house.

Karaim, M., Elsheikh, M., Noureldin, A., & Rustamov, R. B. (2018). GNSS error sources. Multifunctional Operation and Application of GPS; Rustamov, RB, Hashimov, AM, Eds, 69-85.

Landau, H., Vollath, U., & Chen, X. (2003). Virtual reference stations versus broadcast solutions in network RTK—advantages and limitations. In Proceedings of GNSS (pp. 22-25).

Landi, M., Benelli, G. (2016). Protecting crop species from biotic and abiotic constraints in the era of global change: Are we ready for this challenge? American journal of agricultural and biological sciences, 11(2), 51-53.

Langley, R. B. (1997). GPS receiver system noise. GPS world, 8(6), 40-45.

Langley, R. B. (1999). Dilution of precision. GPS world, 10(5), 52-59.

Lemoine, F. G., Kenyon, S. C., Factor, J. K., Trimmer, R. G., Pavlis, N. K., Chinn, D. S., ... & Wang, Y. M. (1998). The development of the joint NASA GSFC and the National Imagery and Mapping Agency (NIMA) geopotential model EGM96.

MAPIR. (2020a) OCN Filter Improves Results Compared to RGN Filter. <https://www.mapir.camera/pages/ocn-filter-improves-contrast-compared-to-rgn-filter> Last visited: 14-01-2020

MAPIR. (2020b) Calibrating Images in MAPIR Camera Control Application <https://www.mapir.camera/pages/calibrating-images-in-mapir-camera-control-application> Last visited: 16-04-2020

MAPIR. (2020c) Rapini (Broccoli Raab) Field (350ft) - November 1st, 2018 <https://www.mapir.camera/pages/rapini-broccoli-raab-field-350ft-november-1st-2018> Last visited: 10-04-2020

Mutanga, O., Dube, T., & Galal, O. (2017). Remote sensing of crop health for food security in Africa: Potentials and constraints. Remote Sensing Applications: Society and Environment, 8, 231-239.

NASA (2020) Landsat 8 <https://landsat.gsfc.nasa.gov/landsat-data-continuity-mission/> Last visited: 31-03-2020

NSGI (2020) RDinfo <https://www.nsgi.nl/rdinfo> last visited 06-03-2020

Pirti, A., Yucel, M. A., & Gumus, K. (2013). Testing real time kinematic GNSS (GPS and GPS/GLONASS) methods in obstructed and unobstructed sites. Geodetski vestnik, 57(3).

Pratt, J., Axelrad, P., Larson, K. M., Lesage, B., Gerren, R., & DiOrio, N. (2013). Satellite clock bias estimation for iGPS. GPS solutions, 17(3), 381-389.

Rieke, M., Foerster, T., Geipel, J., & Prinz, T. (2011). High-precision positioning and real-time data processing of UAV systems. *International Archives of the Photogrammetry, Remote Sensing and Spatial Information Sciences*, 38(1/C22).

Rijswaterstaat (2020) RWS NAPinfo Viewer
<https://geoservices.rijswaterstaat.nl/geoweb51/index.html?viewer=NAPinfo> Last visited 06-03-2020

Rouse Jr, J., Haas, R. H., Schell, J. A., & Deering, D. W. (1974). Monitoring vegetation systems in the Great Plains with ERTS.

Saghravani, S. R., Mustapha, S., & Saghravani, S. F. (2009). Accuracy comparison of RTK-GPS and automatic level for height determination in land surveying. *Masaum Journal of Reviews and Surveys*, 1(1), 10-13.

Sanz-Ablanedo, E., Chandler, J. H., Rodríguez-Pérez, J. R., & Ordóñez, C. (2018). Accuracy of unmanned aerial vehicle (UAV) and SfM photogrammetry survey as a function of the number and location of ground control points used. *Remote Sensing*, 10(10), 1606.

Teunissen, P., & Montenbruck, O. (Eds.). (2017). *Springer handbook of global navigation satellite systems*. Springer.

TU Delft (2020) KOS100NLD Site Information Form
http://gnss1.tudelft.nl/dpga/station/igslog/kos100nld_20190916.log Last visited: 08-04-2020

Uradzinski, M., Kim, D., & Langley, R. B. (2008). The usefulness of Internet-based (Ntrip) RTK for navigation and intelligent transportation systems. In *Proceedings of ION GNSS* (pp. 6-19).

Van Ittersum, M. K., Van Bussel, L. G., Wolf, J., Grassini, P., Van Wart, J., Guilpart, N., ... & Yang, H. (2016). Can sub-Saharan Africa feed itself?. *Proceedings of the National Academy of Sciences*, 113(52), 14964-14969.

Vollath, U., Landau, H., & Chen, X. (2002). Network RTK—concept and performance. In *Proceedings of the GNSS Symposium, Wuhan, China* (pp. 27-30).

Weier, J., & Herring, D. (2000) *Measuring Vegetation (NDVI & EVI)*. NASA Earth Observatory.
https://earthobservatory.nasa.gov/features/MeasuringVegetation/measuring_vegetation_1.php Last visited: 10-02-2020

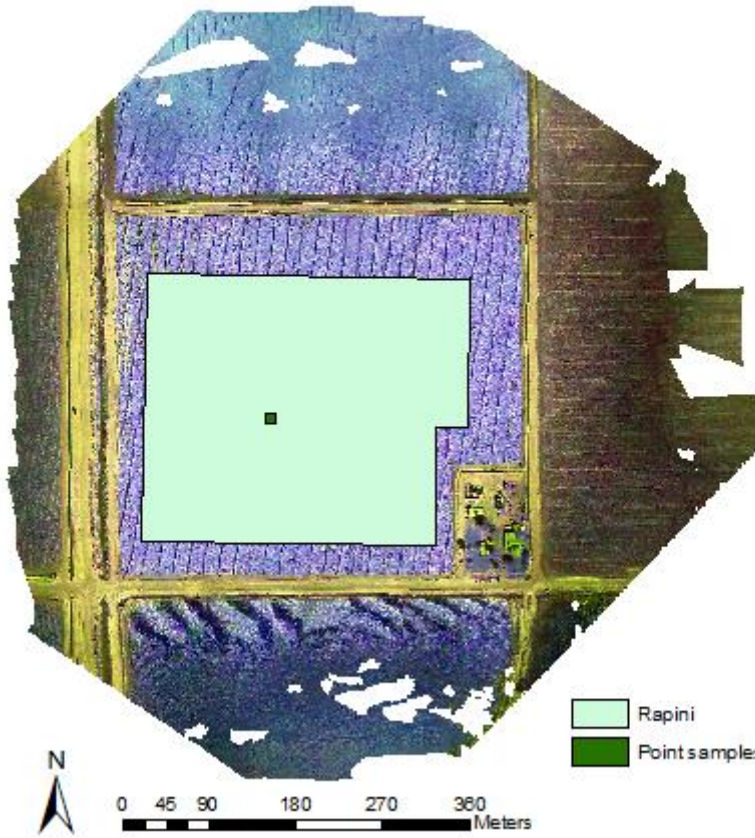
Wierzbicki, D., Kedzierski, M., Fryskowska, A., & Jasinski, J. (2018). Quality Assessment of the Bidirectional Reflectance Distribution Function for NIR Imagery Sequences from UAV. *Remote Sensing*, 10(9), 1348.

Xu, H. (2012). Application of GPS-RTK technology in the land change survey. *Procedia Engineering*, 29, 3454-3459.

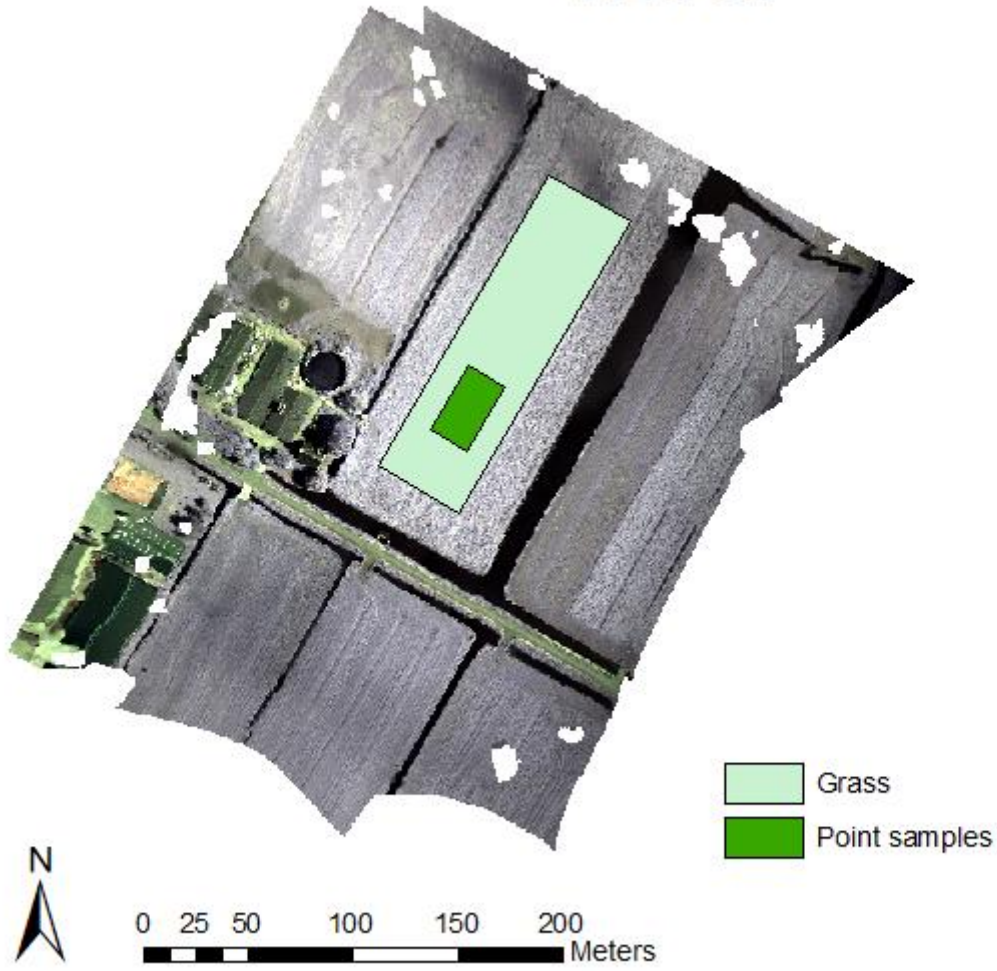
Xue, J., & Su, B. (2017). Significant remote sensing vegetation indices: A review of developments and applications. *Journal of Sensors*, 2017.

Annex I

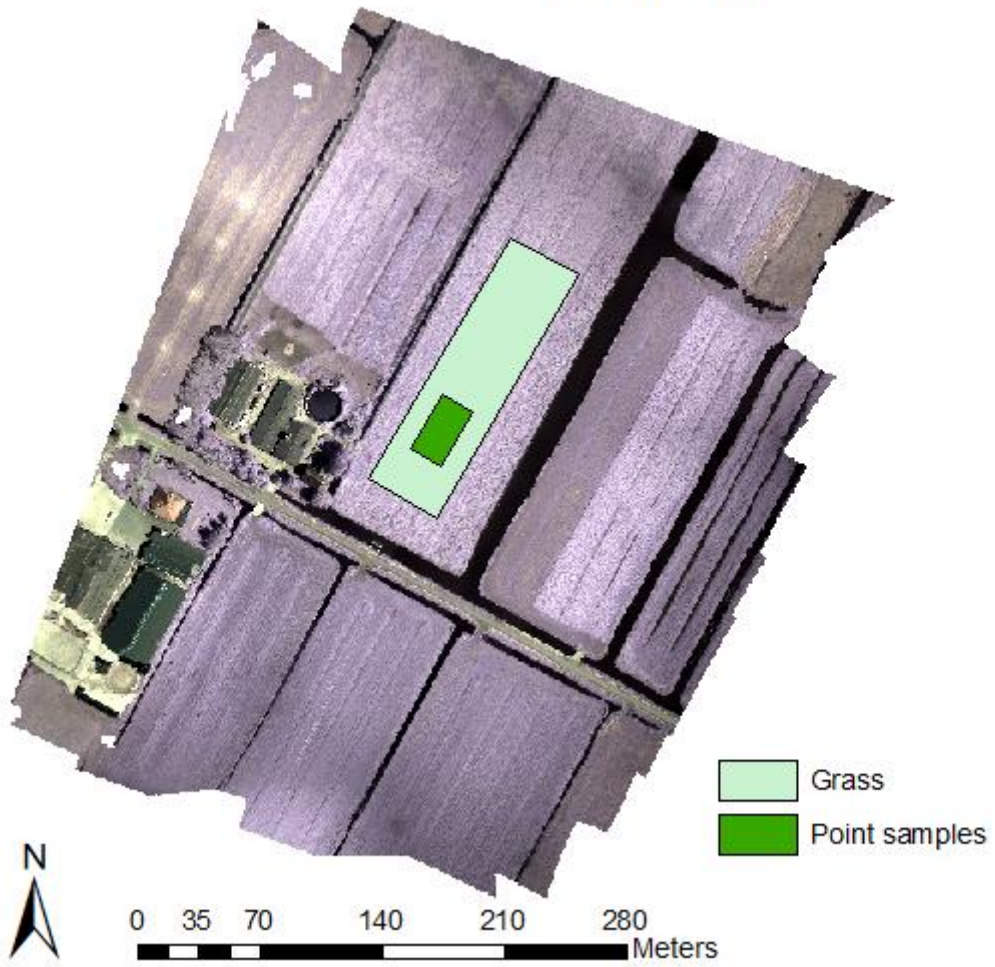
USA



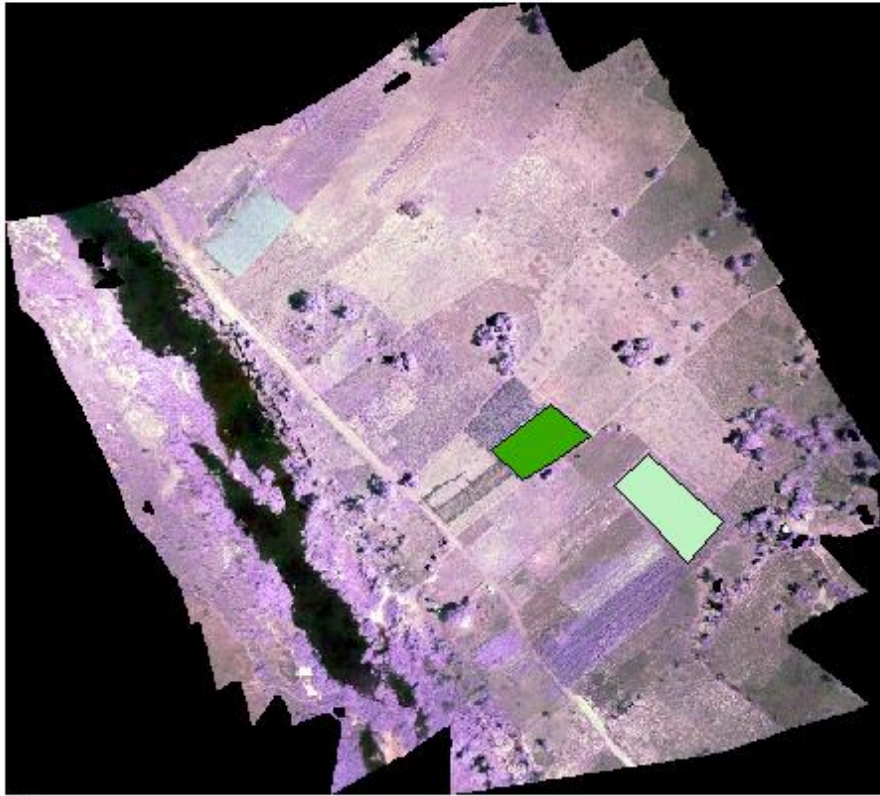
NL F02



NL F03



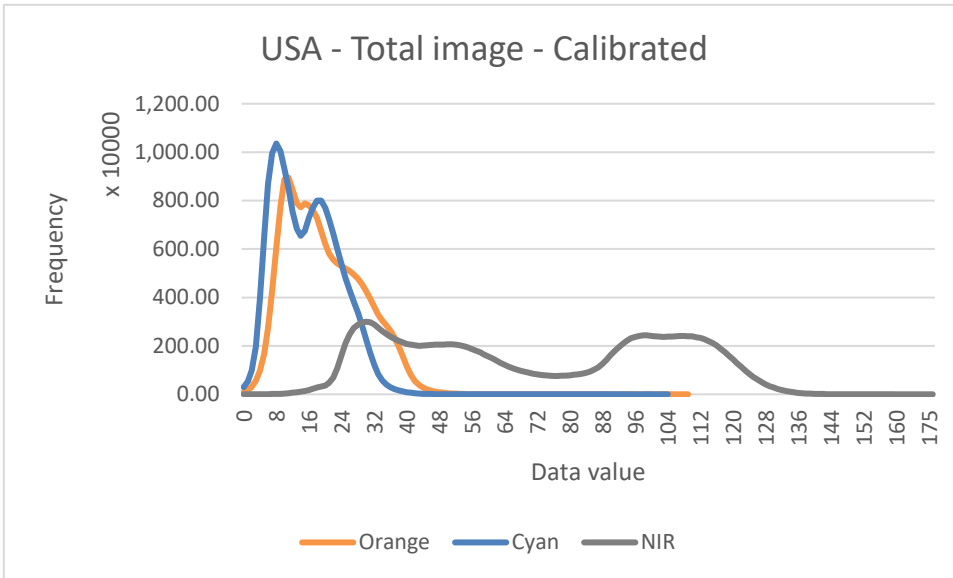
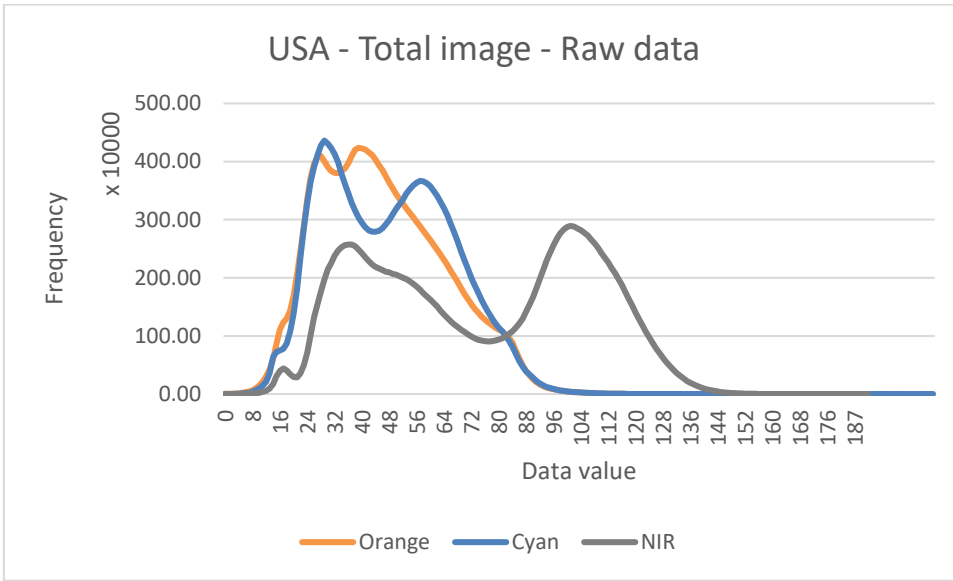
MZ F01

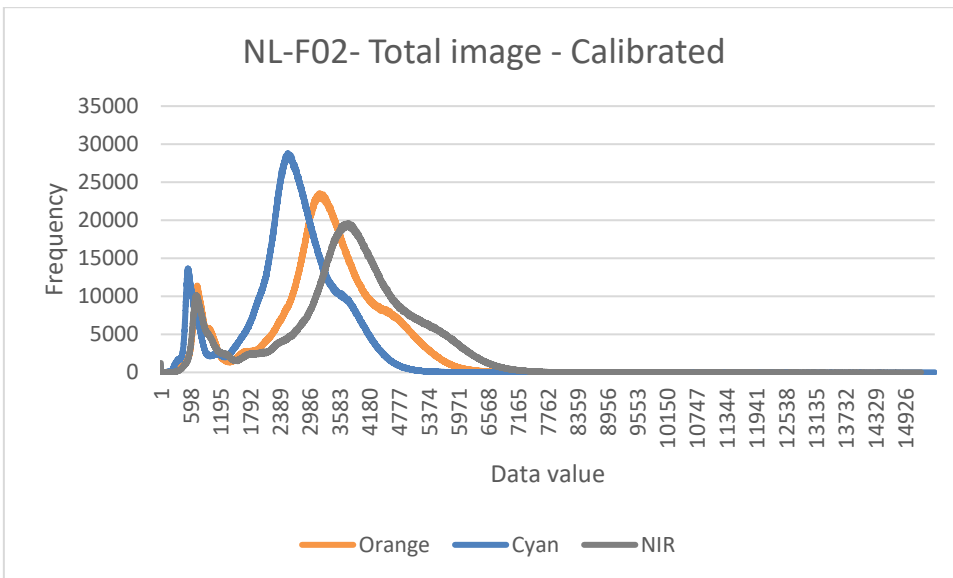
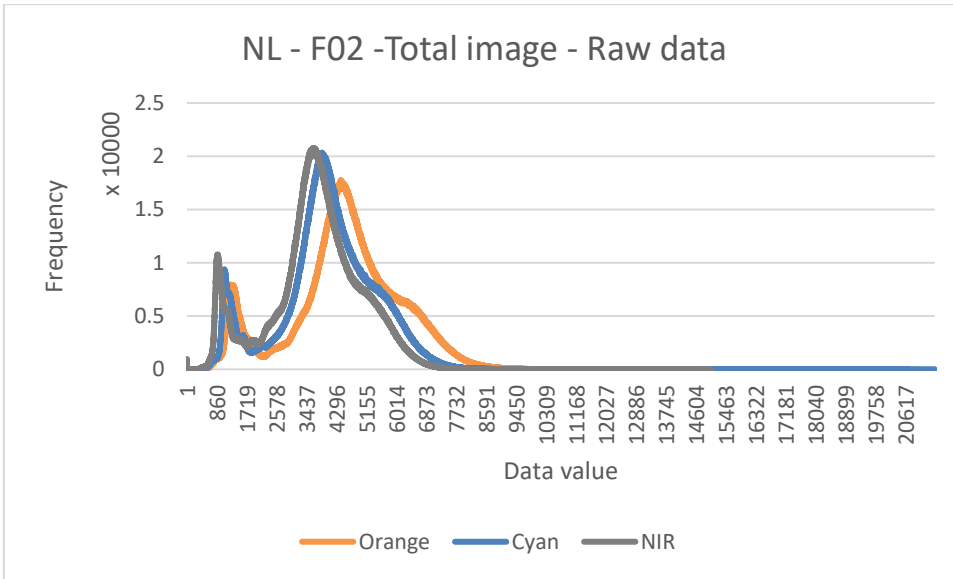


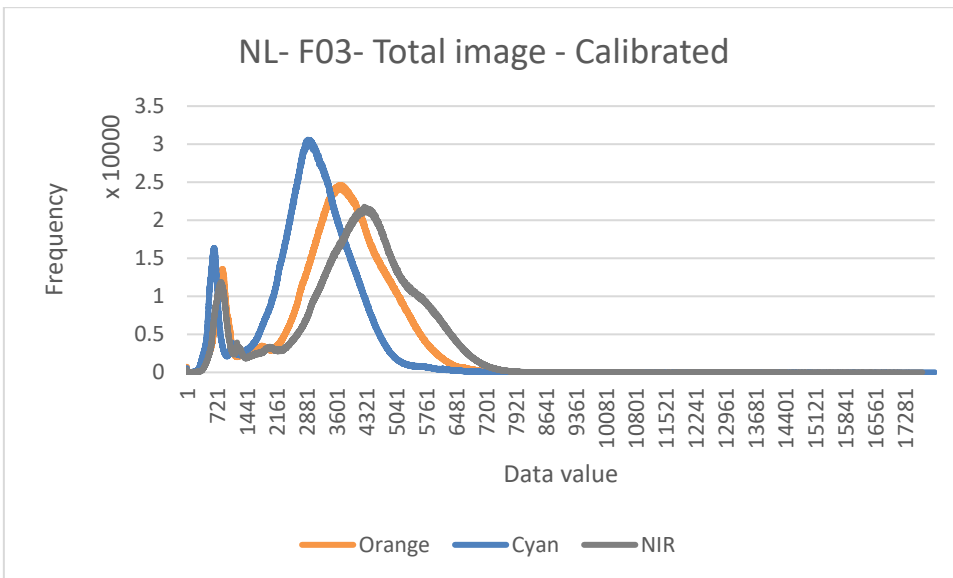
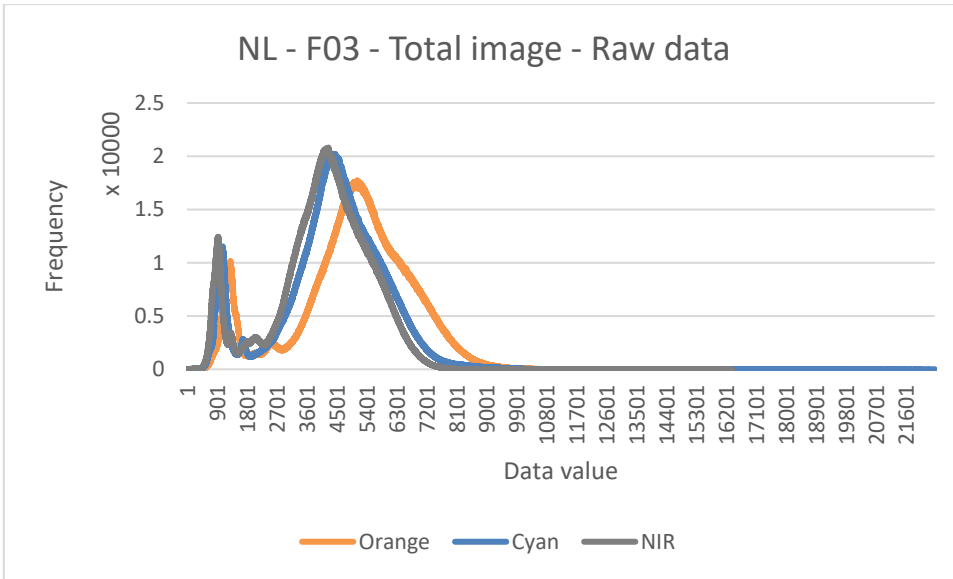
0 25 50 100 150 200 Meters

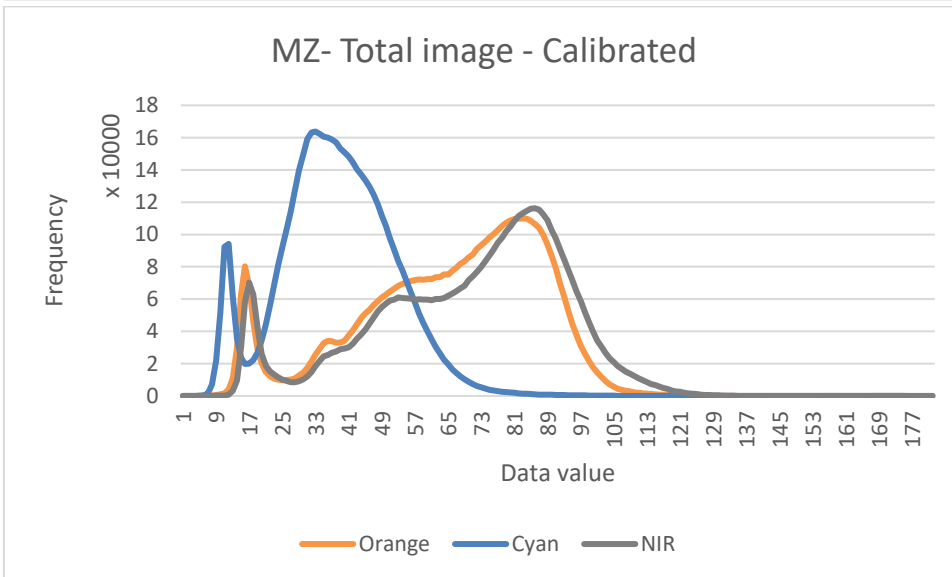
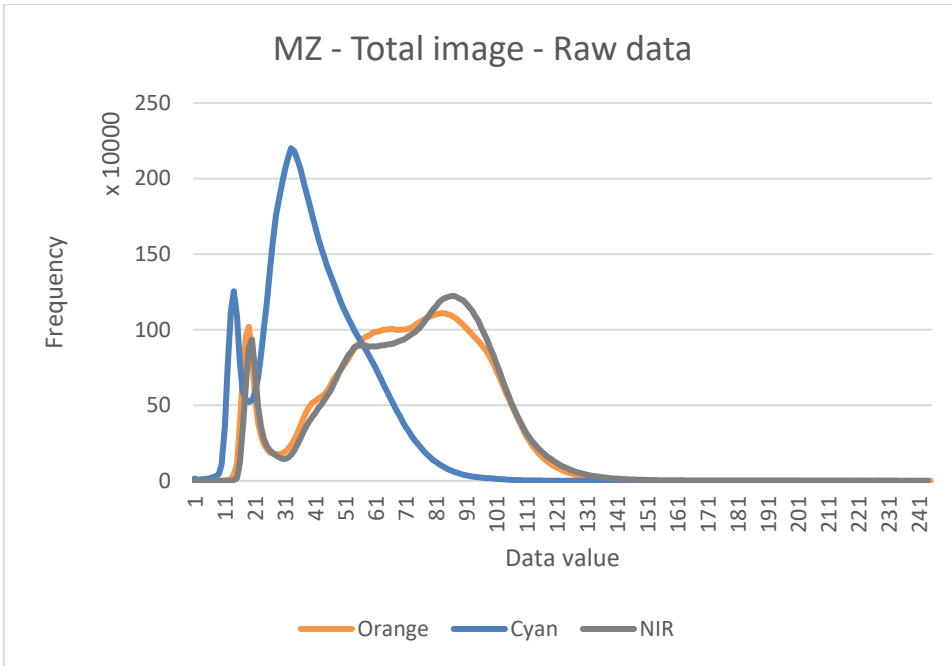
MZ_F01_Crop2
MZ_F01_Crop1

Annex II









Annex III

Point data of Test 1

Point num	POINT_X_A	POINT_Y_A	POINT_Z_Geoid_H	H_ARDUSI	Point_X_topcon	Point_Y_topcon	H_topcon	Line dist	Δ X	Δ Y	Δ Z	
1	174,280.41	444,156.85	54.23198	43.441	10.734	174,280.44	444,156.87	10.742	0.035	0.024	0.026	0.049
2	174,279.12	444,160.01	54.72498	43.441	11.227	174,279.11	444,160.02	11.198	0.015	0.005	0.014	0.086
3	174,277.86	444,163.10	55.11198	43.441	11.614	174,277.85	444,163.13	11.622	0.033	0.011	0.031	0.049
4	174,276.68	444,165.81	54.82598	43.441	11.328	174,276.68	444,165.85	11.343	0.038	0.006	0.038	0.042
5	174,274.81	444,169.16	54.21198	43.441	10.714	174,274.79	444,169.20	10.707	0.041	0.021	0.035	0.064
6	174,280.29	444,173.21	54.19098	43.441	10.693	174,280.30	444,173.23	10.679	0.019	0.004	0.019	0.071
7	174,282.10	444,169.84	55.13498	43.441	11.637	174,282.10	444,169.88	11.637	0.038	0.003	0.038	0.057
8	174,283.91	444,165.77	55.81298	43.441	12.315	174,283.89	444,165.77	12.292	0.020	0.020	0.000	0.080
9	174,285.46	444,162.20	55.14998	43.441	11.652	174,285.45	444,162.24	11.624	0.037	0.006	0.036	0.085
10	174,286.66	444,158.92	54.35798	43.441	10.86	174,286.65	444,158.94	10.855	0.023	0.009	0.021	0.062
11	174,292.33	444,161.76	54.33098	43.441	10.833	174,292.35	444,161.80	10.864	0.042	0.019	0.037	0.026
12	174,291.05	444,164.64	55.05998	43.441	11.562	174,291.07	444,164.66	11.559	0.031	0.021	0.022	0.060
13	174,289.70	444,168.53	55.75098	43.441	12.253	174,289.73	444,168.56	12.237	0.043	0.029	0.032	0.073
14	174,287.53	444,172.86	54.92698	43.441	11.429	174,287.55	444,172.91	11.443	0.059	0.021	0.055	0.043
15	174,286.01	444,176.40	54.06398	43.441	10.566	174,286.01	444,176.40	10.584	0.004	0.003	0.001	0.039
16	174,292.06	444,178.20	54.01698	43.441	10.519	174,292.06	444,178.21	10.504	0.005	0.004	0.004	0.072
17	174,293.17	444,174.82	54.85798	43.441	11.36	174,293.18	444,174.85	11.37	0.039	0.008	0.038	0.047
18	174,294.56	444,170.46	55.76398	43.441	12.266	174,294.55	444,170.47	12.216	0.016	0.009	0.014	0.107
19	174,295.79	444,166.42	55.05698	43.441	11.559	174,295.79	444,166.44	11.558	0.025	0.004	0.024	0.058
20	174,296.52	444,163.34	54.35398	43.441	10.856	174,296.50	444,163.38	10.845	0.040	0.014	0.038	0.068
21	174,298.17	444,162.96	54.37698	43.441	10.879	174,298.17	444,162.97	10.865	0.009	0.000	0.009	0.071
22	174,299.27	444,165.98	55.14998	43.441	11.652	174,299.27	444,166.02	11.649	0.034	0.005	0.034	0.060
23	174,300.56	444,171.43	55.71098	43.441	12.213	174,300.55	444,171.46	12.209	0.031	0.004	0.031	0.061
24	174,300.64	444,176.32	54.69198	43.441	11.194	174,300.65	444,176.36	11.199	0.035	0.001	0.035	0.052
25	174,300.69	444,179.35	54.01998	43.441	10.522	174,300.68	444,179.36	10.506	0.022	0.011	0.019	0.073
26	174,316.28	444,174.98	53.99398	43.441	10.496	174,316.25	444,175.01	10.481	0.040	0.029	0.028	0.072
27	174,313.12	444,171.54	54.82198	43.441	11.324	174,313.09	444,171.56	11.341	0.038	0.030	0.022	0.040
28	174,308.54	444,166.45	55.70898	43.441	12.211	174,308.54	444,166.50	12.198	0.049	0.001	0.049	0.070
29	174,303.56	444,162.35	55.07598	43.441	11.578	174,303.57	444,162.36	11.547	0.006	0.005	0.003	0.088
30	174,300.49	444,160.24	54.22098	43.441	10.723	174,300.50	444,160.23	10.807	0.010	0.007	0.007	0.027
31	174,301.23	444,156.77	54.35698	43.441	10.859	174,301.24	444,156.79	10.831	0.017	0.008	0.015	0.085
32	174,300.33	444,152.34	54.31098	43.441	10.813	174,300.33	444,152.38	10.813	0.038	0.001	0.038	0.057
33	174,298.28	444,149.96	54.29398	43.441	10.796	174,298.29	444,149.98	10.796	0.024	0.006	0.023	0.057
34	174,300.46	444,147.45	55.00998	43.441	11.512	174,300.44	444,147.49	11.531	0.043	0.023	0.036	0.038
35	174,303.62	444,143.95	55.74998	43.441	12.252	174,303.61	444,143.99	12.26	0.047	0.003	0.047	0.049
36	174,306.66	444,141.16	54.84798	43.441	11.35	174,306.64	444,141.20	11.385	0.038	0.011	0.036	0.022
37	174,308.73	444,139.39	54.14098	43.441	10.643	174,308.75	444,139.42	10.645	0.031	0.016	0.027	0.055
38	174,303.14	444,134.52	54.20798	43.441	10.71	174,303.13	444,134.54	10.701	0.025	0.008	0.024	0.066
39	174,301.25	444,136.82	54.85898	43.441	11.361	174,301.26	444,136.83	11.365	0.017	0.009	0.014	0.053
40	174,298.71	444,140.63	55.76398	43.441	12.266	174,298.70	444,140.66	12.276	0.024	0.008	0.022	0.047
41	174,295.95	444,143.58	55.15198	43.441	11.654	174,295.96	444,143.61	11.647	0.033	0.019	0.026	0.064
42	174,293.55	444,146.00	54.33698	43.441	10.839	174,293.56	444,146.03	10.841	0.029	0.003	0.028	0.055
43	174,288.79	444,141.27	54.24198	43.441	10.744	174,288.79	444,141.30	10.777	0.030	0.002	0.030	0.024
44	174,290.94	444,139.52	54.84998	43.441	11.352	174,290.92	444,139.54	11.374	0.025	0.015	0.020	0.035
45	174,293.54	444,137.02	55.47098	43.441	11.973	174,293.55	444,137.05	11.972	0.030	0.004	0.029	0.058
46	174,295.89	444,133.99	54.81398	43.441	11.316	174,295.85	444,134.04	11.34	0.061	0.044	0.043	0.033
47	174,297.42	444,131.15	54.14398	43.441	10.646	174,297.42	444,131.17	10.649	0.021	0.007	0.020	0.054
48	174,303.59	444,150.82	55.19698	43.441	11.699	174,303.58	444,150.86	11.677	0.038	0.011	0.037	0.079
49	174,307.11	444,148.89	55.69398	43.441	12.196	174,307.11	444,148.93	12.189	0.037	0.002	0.037	0.064
50	174,311.06	444,147.06	54.71898	43.441	11.221	174,311.05	444,147.09	11.225	0.029	0.017	0.023	0.053
51	174,313.37	444,145.48	54.10198	43.441	10.604	174,313.34	444,145.54	10.576	0.067	0.031	0.060	0.085
52	174,318.28	444,154.02	54.09498	43.441	10.597	174,318.25	444,154.03	10.585	0.025	0.024	0.003	0.069
53	174,315.16	444,155.43	54.73998	43.441	11.242	174,315.16	444,155.44	11.232	0.017	0.007	0.016	0.067
54	174,310.10	444,156.50	55.60798	43.441	12.11	174,310.11	444,156.49	12.08	0.013	0.003	0.013	0.087
55	174,305.19	444,156.81	55.07498	43.441	11.577	174,305.19	444,156.82	11.557	0.008	0.006	0.005	0.077

Point data of Test 3

	Line Distance				ΔX		
	1	2	3		1	2	3
Point 1	2.608	0.054	0.054	Point 1	0.103	0.041	0.036
Point 2	2.599	0.036	0.044	Point 2	0.110	0.027	0.032
Point 3	2.603	0.042	0.037	Point 3	0.123	0.024	0.034
Point 4	2.591	0.040	0.033	Point 4	0.095	0.024	0.018
Point 5	2.603	0.040	0.015	Point 5	0.081	0.028	0.013
Point 6	2.610	0.043	0.039	Point 6	0.109	0.036	0.027
Point 7	2.632	0.015	0.021	Point 7	0.115	0.014	0.018
Point 8	2.606	0.069	0.032	Point 8	0.076	0.030	0.007
Point 9	2.622	0.046	0.030	Point 9	0.113	0.039	0.028
Point 10	2.605	0.060	0.037	Point 10	0.121	0.059	0.036
Point 11	2.604	0.038	0.031	Point 11	0.102	0.021	0.022
Point 12	2.582	0.040	0.040	Point 12	0.108	0.012	0.016
Point 13	2.616	0.032	0.011	Point 13	0.113	0.029	0.009
Point 14	2.617	0.040	0.016	Point 14	0.097	0.031	0.013
Point 15	2.583	0.037	0.030	Point 15	0.050	0.023	0.012
Point 16	2.609	0.031	0.026	Point 16	0.100	0.004	0.014
Point 17	2.602	0.032	0.027	Point 17	0.097	0.023	0.012
Point 18	2.610	0.034	0.023	Point 18	0.094	0.010	0.016
Point 19	2.611	0.047	0.043	Point 19	0.093	0.028	0.027
Point 20	2.613	0.032	0.026	Point 20	0.038	0.032	0.026
Point 21	2.603	0.048	0.047	Point 21	0.101	0.027	0.019
Point 22	2.609	0.015	0.012	Point 22	0.102	0.002	0.001
Point 23	2.611	0.028	0.019	Point 23	0.103	0.020	0.009
Point 24	2.591	0.030	0.046	Point 24	0.102	0.009	0.000
Average	2.606	0.039	0.031	Average	0.098	0.025	0.019
Max	2.632	0.069	0.054	Max	0.123	0.059	0.036
Min	2.582	0.015	0.011	Min	0.038	0.002	0.000
std	0.011	0.012	0.012	std	0.020	0.012	0.010

	ΔY				ΔZ		
	1	2	3		1	2	3
Point 1	2.606	0.035	0.041	Point 1	0.840	0.121	0.123
Point 2	2.596	0.025	0.030	Point 2	0.832	0.133	0.115
Point 3	2.600	0.035	0.017	Point 3	0.805	0.150	0.153
Point 4	2.589	0.032	0.028	Point 4	0.822	0.133	0.140
Point 5	2.602	0.029	0.007	Point 5	0.795	0.152	0.134
Point 6	2.608	0.025	0.028	Point 6	0.811	0.124	0.116
Point 7	2.630	0.005	0.011	Point 7	0.819	0.169	0.138
Point 8	2.605	0.062	0.031	Point 8	0.801	0.172	0.128
Point 9	2.620	0.025	0.010	Point 9	0.808	0.130	0.125
Point 10	2.602	0.013	0.008	Point 10	0.839	0.149	0.111
Point 11	2.602	0.031	0.021	Point 11	0.808	0.153	0.127
Point 12	2.580	0.038	0.036	Point 12	0.826	0.087	0.092
Point 13	2.613	0.014	0.006	Point 13	0.844	0.112	0.097
Point 14	2.615	0.025	0.010	Point 14	0.815	0.137	0.137
Point 15	2.582	0.029	0.027	Point 15	0.800	0.131	0.131
Point 16	2.607	0.031	0.022	Point 16	0.804	0.142	0.142
Point 17	2.600	0.023	0.024	Point 17	0.820	0.128	0.106
Point 18	2.609	0.032	0.017	Point 18	0.811	0.141	0.122
Point 19	2.609	0.038	0.034	Point 19	0.824	0.135	0.136
Point 20	2.613	0.005	0.001	Point 20	0.727	0.134	0.121
Point 21	2.601	0.040	0.043	Point 21	0.799	0.146	0.140
Point 22	2.607	0.015	0.012	Point 22	0.817	0.150	0.151
Point 23	2.609	0.019	0.016	Point 23	0.820	0.140	0.116
Point 24	2.589	0.028	0.046	Point 24	0.847	0.149	0.100
Average	2.604	0.027	0.022	Average	0.814	0.138	0.125
Max	2.630	0.062	0.046	Max	0.847	0.172	0.153
Min	2.580	0.005	0.001	Min	0.727	0.087	0.092
std	0.011	0.012	0.012	std	0.023	0.017	0.016

7 User guide ArduSimple RTK System with WiFi connection

7.1 Necessary material

- 2 ArduSimple boards
- 2 antennas
- 1 WiFi NTRIP Master module
- 1 jumper cable
- 2 USB / micro USB cables
- 1 USB to micro USB adapter
- 1 mobile phone with mobile data
- SW Maps (Android app)
- 1 laptop with U-center software (Windows only)
- Field notebook
- CD/metal plate

7.2 The RTK principle

The RTK technology consist of at least two Global Navigation Satellite Systems (GNSS) receivers. One receiver is located at a known static location, this is referred to as the base station. The other receiver(s), the rover, is used to determine an unknown position. The rover can be used in a static or mobile state. The basic setup of an RTK system can be seen in Figure 1. The base station sends correction data with an internet connection to the rover. The corrections are based on the location error of the base station. It is assumed that the rover station will have similar error sources as the base stations, the location of the rover will therefore be corrected with that error. This system provides real-time correction, which enables up to centimeter-level accuracy.

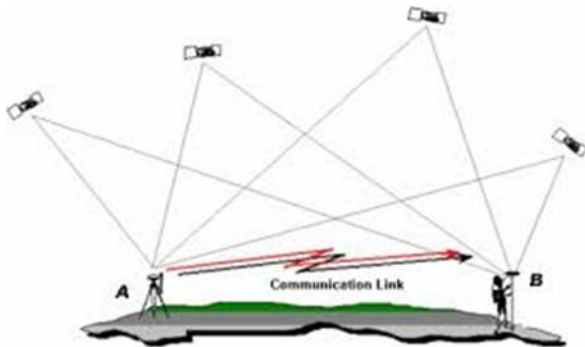


Figure 11 RTK setup, where A is the base station and B is the rover station.

NOTE: Within the RTK system there will be no corrections for multipath and receiver noise errors. It is therefore important to place the base station and the rover under clear sky conditions (e.g. no obstructions of buildings). A CD or metal plate can be used to reduce the multipath reflectance from the ground.

7.3 Base station

As mentioned above an RTK system works with a base station and a rover station. The rover will always be operated by you as a user. But there are two options for the base station: using your own base station

or using a base station which is already set-up. However, it is only possible to use the rover without setting up your own base station if you have access to nearby base stations.

When using your own base station proceed with this chapter, else skip this chapter and start at '4. Rover'.

7.4 Base station set-up

The components of the base station can be seen on Figure 2 and the base station set-up should look like Figure 3. This is achieved by executing the following steps:

1. Connect the WiFi NTRIP Master module to the ArduSimple board, by pressing the module on to the XBee socket.
2. Connect the u-blox antenna to the ArduSimple board. This does **not** require any tools, just turn with your fingers the cable of the antenna on to the gold antenna port on the ArduSimple board.
3. Place the antenna on the CD/metal plate and put the antenna at a secure location with a clear sky view, **where it will not be moved.**
4. Power the ArduSimple board, by connecting a power source with a USB to micro USB cable to the ArduSimple board by preferably using the 'power + GPS' port. **If WiFi NTRIP Master module and/or the antenna are not connected before the ArduSimple board is powered, it is possible they are not recognized.** Therefore, it is important to connect them first before powering the board. This is also the case for the elements which need to be connected to the rover ArduSimple board.

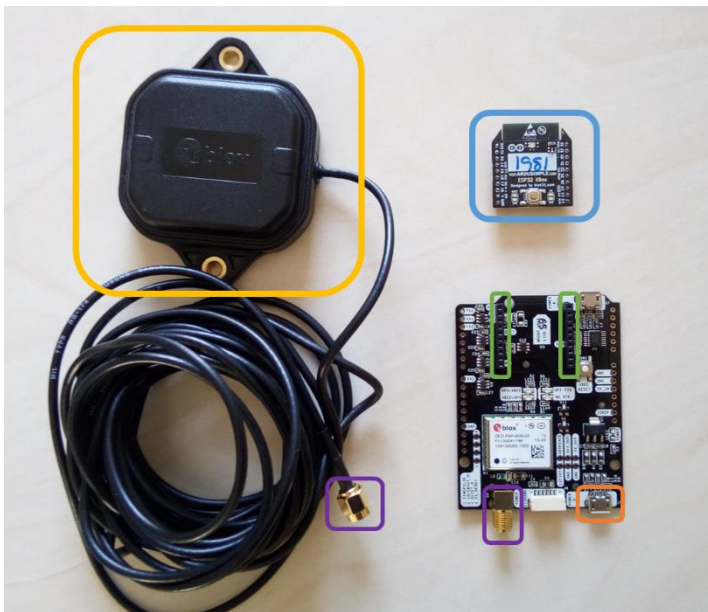


Figure 2 The components of the base station. The element in the yellow box is the antenna. The elements in the purple squares need to be connected to link the antenna to the system board. The component in the bleu box is the WiFi NTRIP Master module, this needs to be pressed onto the XBee socket (green boxes). The board is powered with the USB power socket of the orange box.

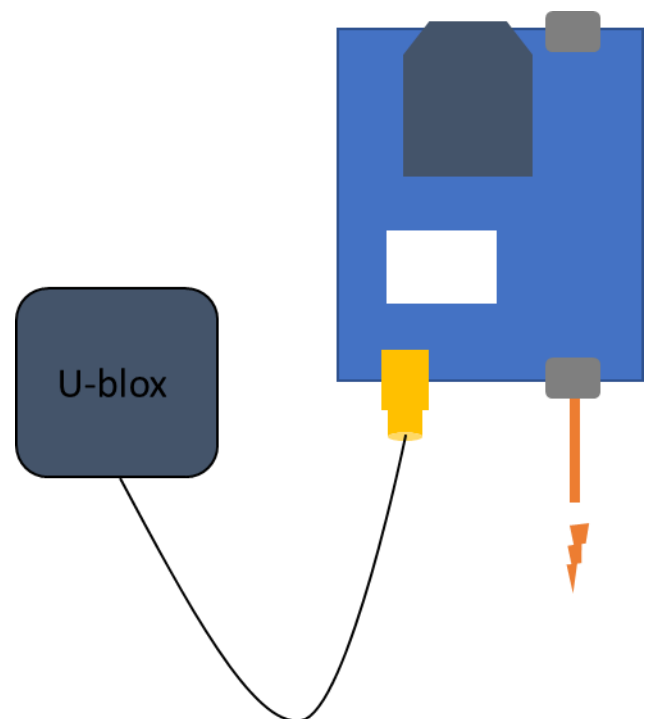
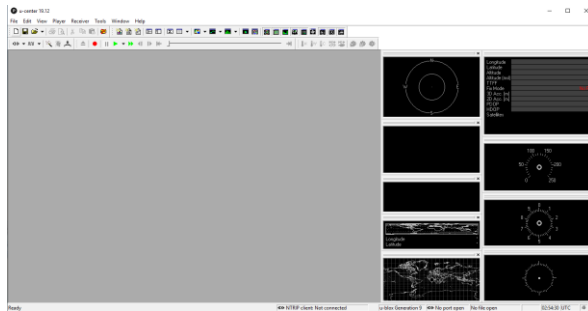


Figure 3 Schematic representation of the base station set-up

7.5 U-center settings

Connect the base station with a USB/micro-USB cable to a laptop with U-center software (can be downloaded for free here: <https://www.u-blox.com/en/product/u-center>). The laptop serves now as the power source. Open U-center. A screen similar to the following figure will appear.



The task bar consists of several elements. The elements which will be used will be described below.



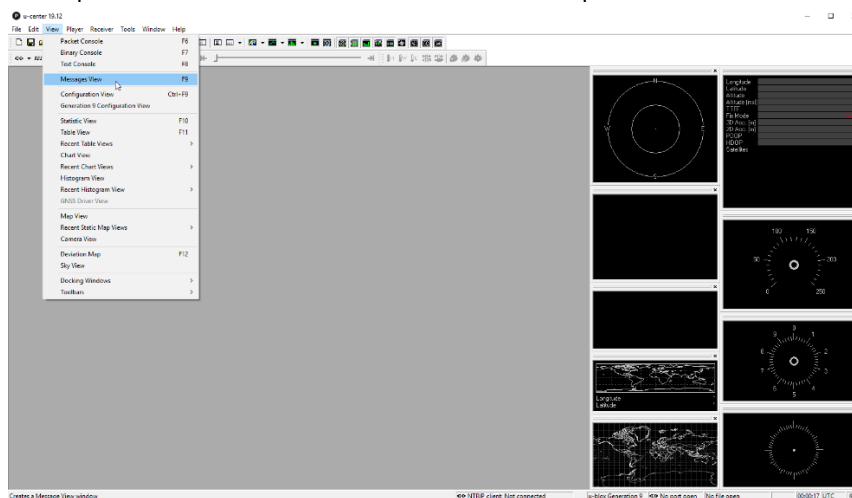
Press the left button of the above displayed buttons to connect a board to U-center. Select the port to which the board is connected to the laptop. When the board is connected, the button will turn green. The right button can be used to change the Baud rate; which is the number of signal changes that occur in one second. **Set this to 115`200.**

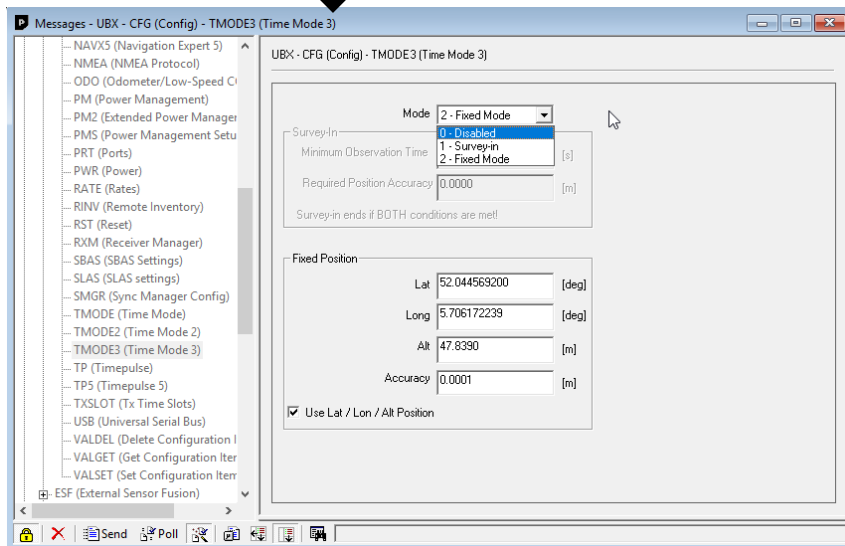
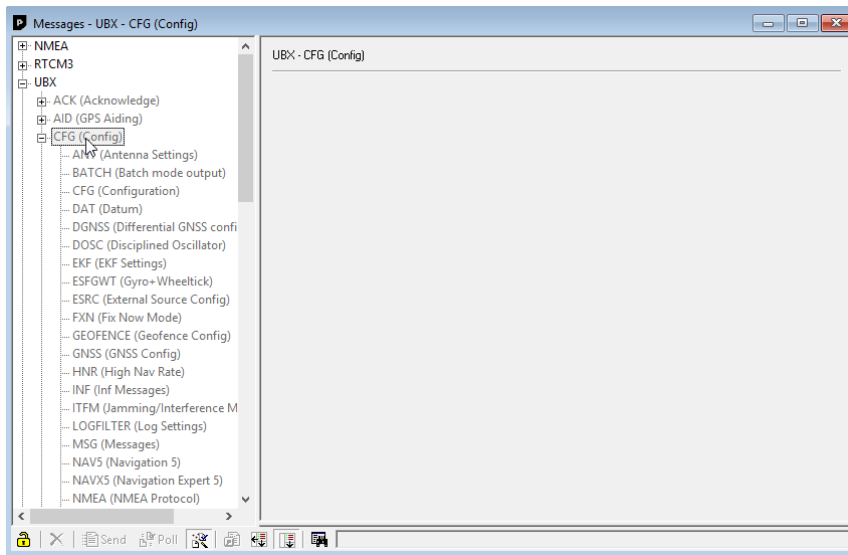


In the section above it is possible to select a variety of graphs to display. When hovering over the symbols it will indicate which graph type it represents. The ones to select depend on the purpose of the research, however most often the 'Data View', 'satellite levels', 'satellite levels history' and 'watch' are useful to display.

The base station can determine its own location, or the user can provide the location if this is known. It is preferred to use a known location, since letting the base station determine its own location is less accurate. To select the required method regarding the base station's location, follow the next steps:

1. Go to View → Message View → UBX → CFG (Config) → TMODE3 (Time Mode 3). Select at 'Mode' either '1- Survey-in' for the base station to locate its own position or '2- Fixed Mode' to provide the known location of the base stations position.





2. When '1- Survey-in' was selected you can provide a desired 'Minimum Observation Time' and 'Required Position Accuracy'. The Survey-in ends if both of these conditions are met and the location will be locked in. After this, the base station can send the correction data. The default settings for 'Survey-in' are 120s for minimum observation time and 2.500m for required position accuracy. Keep in mind when lowering the required position accuracy, it will take longer until the base station can start sending correction data (and therefore, it will take longer before you can start your measurements).
3. If '2- Fixed Mode' is selected, the location needs to be provided under 'Fixed Position'. This can be in X/Y/ Z or Latitude/Longitude/ Altitude. It is assumed you enter the ellipsoid height as Z or altitude values. For more information regarding elevation values see '5. Height in GNSS'
4. At the end of the 'Mode' selection and entering the required information, you need to click 'Send' (left bottom corner) to confirm the selection of required location method. To save the selection go to UBX- CFG -CFG, select all devices (0-BBR, 1-Flash, 2-I2C-EEPROM, 4-SPI-FLASH) and press 'Send'. Now your base station is ready for use.
5. When the selection was made to use the '1- Survey-in' mode, the base station will need a few minutes/hours to calculate its position. Let the base station do this before proceeding to the next

step '3.3 NTRIP network'. If the '2- Fixed Mode' was selected, the base station will immediately be (after step 4) ready for use.

7.6 NTRIP network

A Network Transport of RTCM via Internet Protocol (NTRIP) network will be set-up in order to connect the base station to a rover. This is done as follows. Connect your laptop to the WiFi signal the base station transmits, which is: 'ESP_XBEE_995B09'. Go to '192.168.4.1' in an internet browser. The ESP32 Xbee Configuration page will appear, which looks like Figure 4.

ESP32 Xbee Config v0.4.3

Adjust the settings below and then click on "Submit". The device will restart with the new settings applied. If you have adjusted WiFi settings the device may be moved onto a new IP address, or require you to reconnect to its access point.

Admin (this page)

Auth method: Open | Username: | Password: |

UART (main communication)

UART controller: UART 0 | UART 1 | UART 2 | TX pin: 1 | RX pin: 3

Baud rate: 115200 | Data bits: 8 | Stop bits: 1 | Parity: Disabled

Log forward: Print | Flow control: RTS | CTS | RTS pin: 14 | CTS pin: 33

WiFi hotspot ESP_XBee_995B09 (OPEN) / 192.168.4.1 / 1 device

SSID: ESP_XBee_995B09 | Security: Hidden | Open

Gateway and subnet: 192.168.4.1 / 24 | Min/max IP: 192.168.4.1 - 254

WiFi Not Connected

SSID: AndroidAP6a3e | Password: | Scan

Submit Query

NTRIP client

Socket server

Socket client

NTRIP server

Host and port: rtk2go.com : 2101 | Mountpoint: Base_FW_WAG

Username: | Password: |

Figure 4 The ESP32 Xbee configuration page

1. Fill in the SSID for the WiFi hotspot. This SSID is the name of the network: 'ESP_XBEE_995B09'.
2. Turn on the data and make a hotspot on the mobile phone. Fill in the name and the password of this hotspot at the heading 'WiFi'.
3. Press 'Submit Query'.
4. Fill in the **NTRIP server** section with the following data.
Host: rtk2go.com
Port: 2101
Mountpoint: Base_FW_WAG (this is case sensitive and must match to be used)
Password: hwpX8WrD (also case sensitive)
Username can remain empty.
5. Press 'Submit Query' again.

Now your base station is ready to be connected to a rover.

7.7 Rover

7.7.1 Rover set-up

The components of the rover can be seen on Figure 5 and the base station set-up should look like Figure 6. This is achieved by executing the following steps:

1. Connect the 'TX' and 'RX' ports on the ArduSimple board with a jumper cable.
2. Connect the u-blox antenna to the ArduSimple board. Do this by turning (with your fingers) the cable of the antenna on to the gold antenna port on the ArduSimple board.
3. Connect a power source with a USB to micro USB cable to the ArduSimple board, use preferably the 'power + GPS' port. Multiple LED lights will turn on. This power source can be a laptop or a mobile phone.

The Rover can be connected to a laptop or to a mobile phone. Both options will be explained, however it is suggested to mainly use the mobile phone connection.

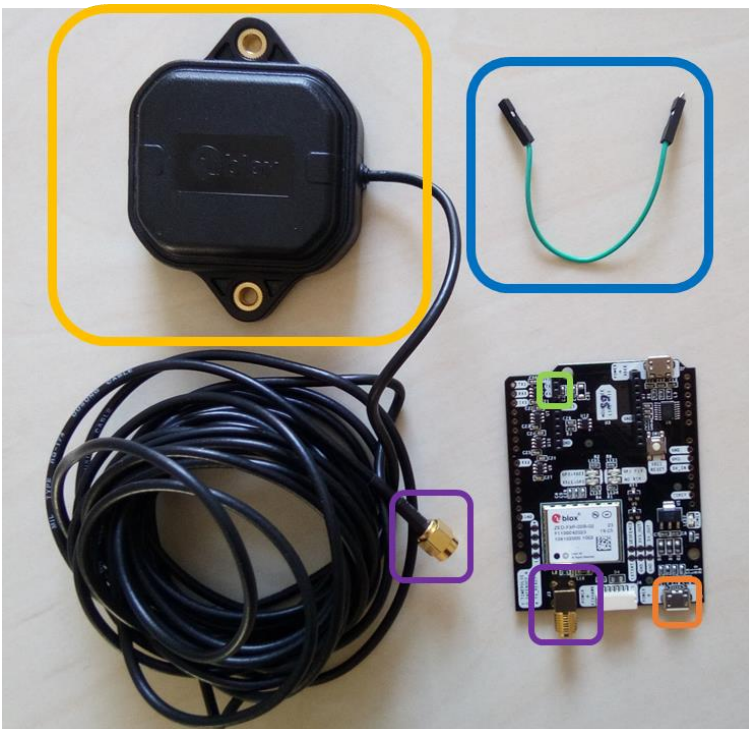


Figure 5 The components of the base station. The component in the yellow box is the antenna. The elements in the purple squares need to be connected to link the antenna to the system board. The component in the blue box is the jumper cable, this is used to connect the TX and RX ports (located in the green box). The board is powered with the USB power socket of the orange box.

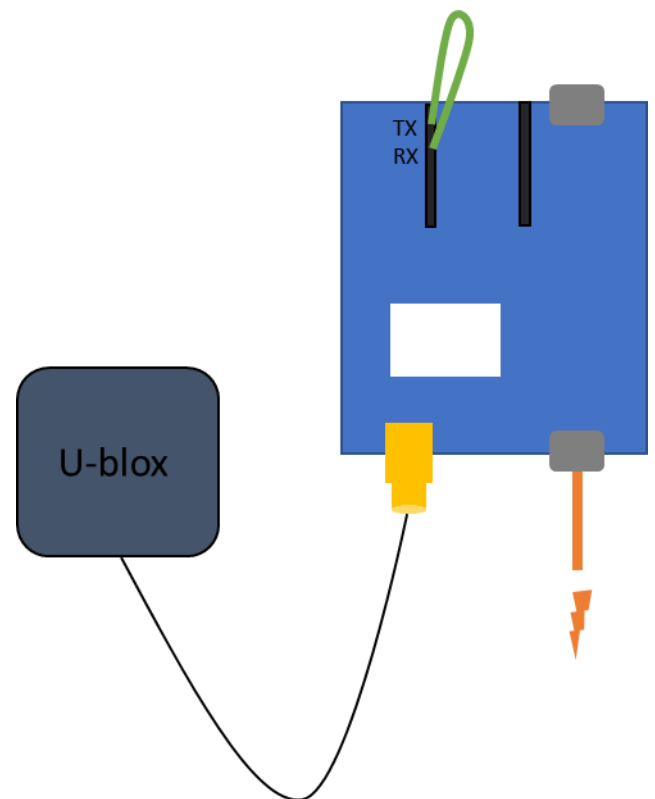
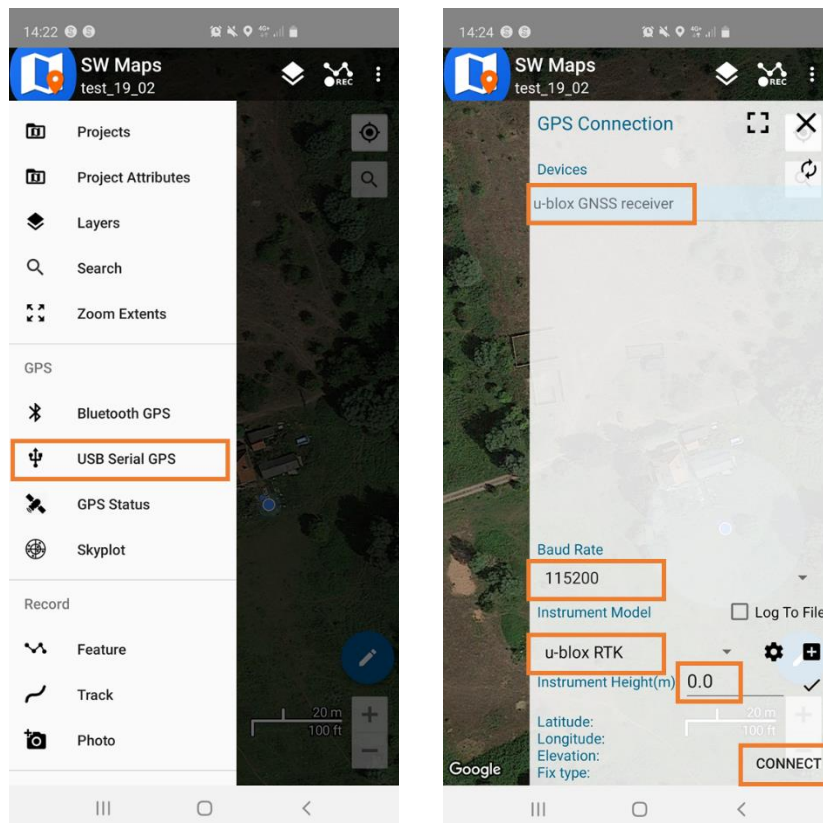


Figure 6 Schematic representation of the rover set-up

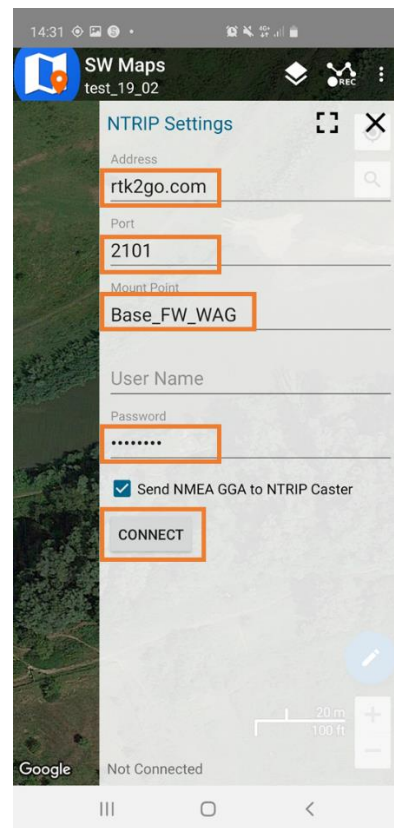
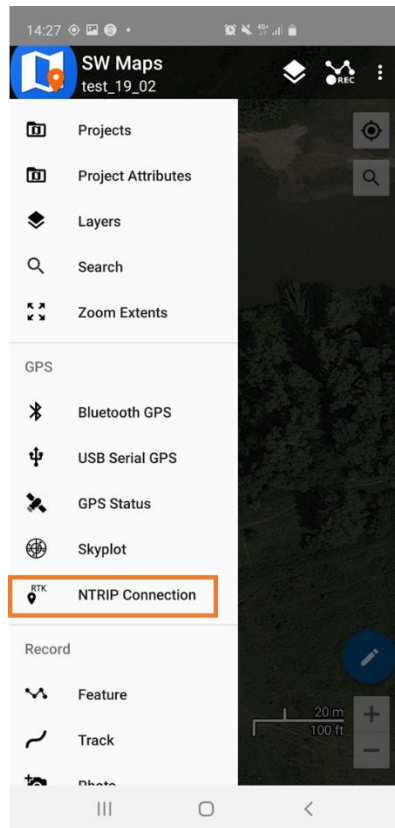
7.7.2 Mobile phone

Make sure the Android app 'SW maps' is installed on the mobile phone (<https://play.google.com/store/apps/details?id=np.com.softwel.swmaps&hl=en>).

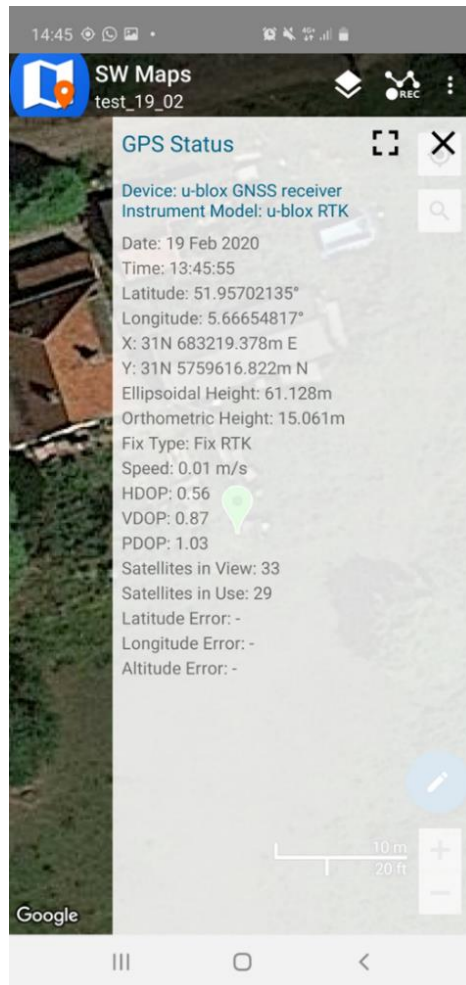
1. Connect the rover to the mobile phone with the usb/micro-usb cable and usb to micro usb adapter. **Put this adapter on the side of the phone**, not on the site of the ArduSimple board.
2. Open SW maps and begin a new project. Give this project an appropriate name.
3. Go to the menu at the upper left corner (the SW map icon) and click on 'USB serial GPS'. Select the correct device. Set the Baud rate on 115200. The instrument model should be 'u-blox RTK' and provide the correct instrument height. Click on 'Connect'.



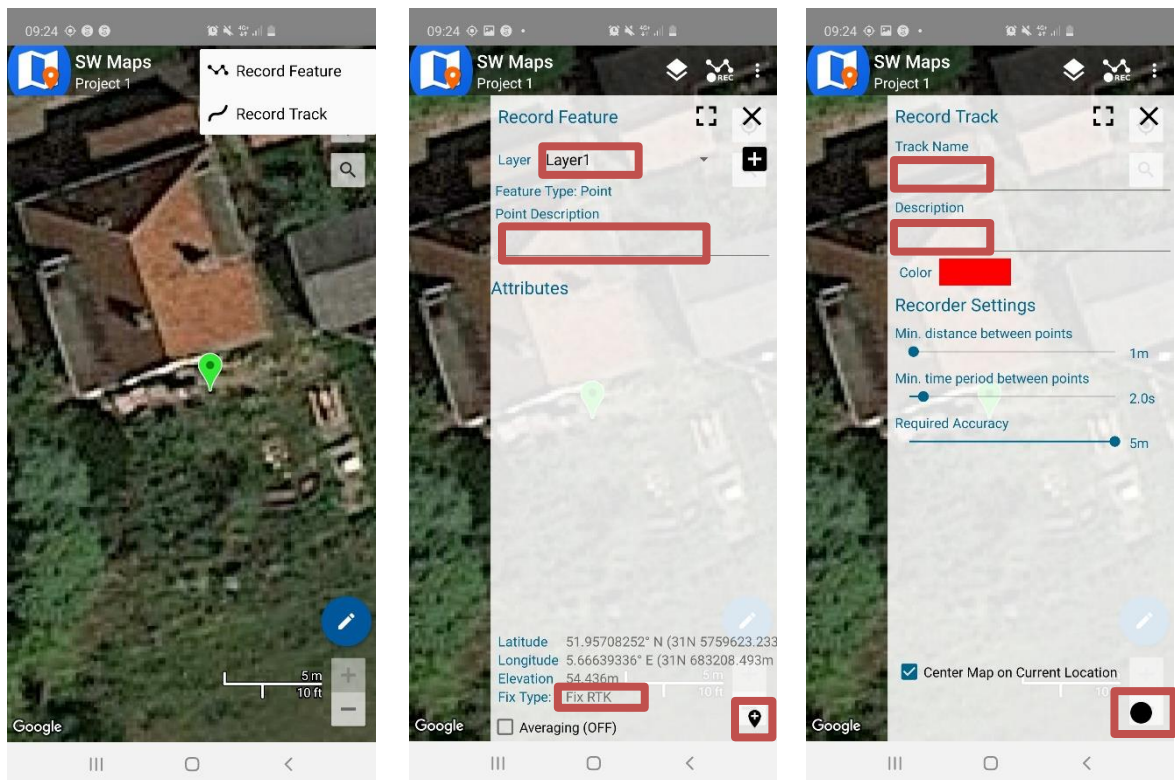
4. Go back to the menu and select 'NTRIP Connection'. Fill in the NTRIP Settings with the following data if you are using the base station described above (if not, fill in the address/information of the desired base station, more information on this can be found in Chapter '6.Using an external base station').
 - Address: rtk2go.com
 - Port: 2101
 - Mount point: Base_FW_WAG (this is case sensitive and must match to be used)
 - Password: hwpX8WrD
 - Username can remain empty. Enable the 'Send NMEA to NTRIP caster'.
 - Click on 'Connect'.



5. Check the 'GPS status' in the menu. If there is an RTK connection the 'Fix type' will be 'Float RTK' or 'Fix RTK'. The 'NO RTK' led on the rover board will also turn off. The location pin will also change colors according to the Fix type, which is an indication on the accuracy.
 - Green pin: Fix RTK (2 cm accuracy)
 - Orange pin: Float RTK (20 cm accuracy)
 - Blue pin: DGPS (2.5 accuracy)
 - Red pin: Single (3m accuracy)



6. Now you are ready to start recording tracks or point features! Place the antenna (with the cd/ metal plate underneath) of the rover on a point of interest. Click on the 'REC' icon. Here you have the choice of recording point features or a track:



- a. Features: When the selection was made to recorded features, make a layer or select a layer you already created. The points will be added to this layer. You can add a description per point (not required). When the fix type has the required status, you can press the 'add point' button. There is no need to close and reopen the window to add an additional point, just press the 'add point' button again. It is advised to wait until you have a 'Fix RTK' before you record your point. This can take a couple of sec/min per point.
 - b. Track: When recording a track, you need to name it and you can add a description. You can also select the minimum distance between points and the minimum time period between point. In addition, the required accuracy can be selected. You start recording your track if you press the black dot at the right bottom corner. Press the black square when you are done recording.
 - c. You can have multiple layers and/or tracks within one project, so record as many features and tracks you need.
6. It is also possible to add photos to your data. This can be done by selecting 'Take New Photo' in the menu. The photos will be linked to the locations where you took them.
 7. When done recording the points or tracks, it is possible to export them. Go to the menu and press 'Export'. Here it is possible to select a variety of export datafile types. Select the one required. It is also possible to 'share' the recorded data via email (or other networks).

7.7.3 Laptop

If you are using the laptop connection make sure the base station is disconnected but has still a power source. This can be the laptop, but preferably another source, else you cannot move. It is also possible to use two laptops, one for the base station and one for the rover.

1. Connect the rover to the laptop. Connect the rover in U-center and set the Baud rate to 115`200.
2. Go to 'Receiver' → 'NTRIP Client...'
3. Fill in 'rtk2go.com' for the Address and '2101' for Port (or the information of an external base station).

4. Click on 'Update source table' and select 'Base_FW_WAG' and press OK (or the information of an external base station).
5. The Fix mode in the data view will change to 3D/DGGNS/FLOAT or 3D/DGGNS/FIX. The 3D/DGGNS/FLOAT status indicates a lower accuracy (20cm) than the 3D/DGGNS/FIX status, which indicates a higher accuracy (2cm)
6. Start recording your points.

7.8 Height in GNSS

The GNSS technology has many positive aspects, however a weakness of the system is that the initially indicated heights are not physically meaningful. The initially indicated is a mathematical simplified representation of the shape of the earth, also referred to as the ellipsoidal height. It is not a relative height to a reference surface; this reference surface is for instance in the Netherlands the Normaal Amsterdams Peil (NAP). This referenced height is also referred to as orthometric height. In Figure 7 a schematic overview is given how the ellipsoidal height and the geoidal heights relate to each other. The orthometric height is calculated by subtracting the geoid height from the ellipsoidal height.

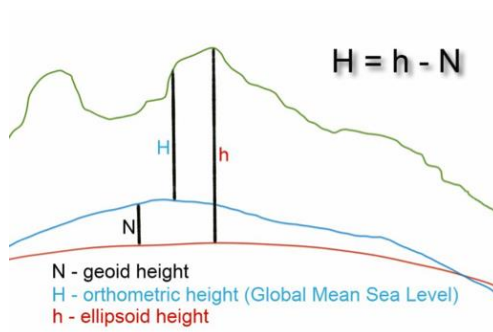


Figure 12 A schematic overview of the geoid height (N), the orthometric height (H) and the ellipsoidal height (h). Source: unavco, 2020

The geoid height can be obtained from a regional gravimetric geoid model or a global geopotential model. A widely used global geopotential model is the EGM96 model (Lemoine et al., 1998). This model is also the default model the ArduSimple RTK setup. Besides global geopotential models there are also regional gravimetric models. These models can provide a higher level of detail and more accurate data.

When working with the SW Maps app the elevation value which will **be exported is the ellipsoidal height and not the orthometric height**. Keep in mind that this ellipsoidal height needs to be corrected in the exported data in order to get the orthometric height. There are multiple options dealing with this:

Working with an own base station:

When working with your own base station there is an option to avoid the need to correct the exported elevation value. When you have selected to work with the '2- Fixed Mode' (see step 3 under U-center settings) you need to provide a 'Z' or 'Altitude' value. It is assumed you provide the ellipsoidal height; however, this is usually not known and therefore there is a need to correct the known orthometric height first. To work around this, it is also possible to provide the orthometric height at the '2- Fixed Mode' settings. In this case, the indicated the ellipsoidal height in SW maps will actually be the value of the orthometric height. This also means that the exported elevation values do not require to be corrected anymore.

Working with an external base station:

Within the app you can see you can see both the ellipsoidal height and the orthometric height. **Note at the beginning of your measurements both the ellipsoidal and orthometric height down.** Subtracting the orthometric height from the ellipsoid height gives you the geoid height, the value you need to correct the exported ellipsoidal heights. Keep in mind that the geoid height varies per location, so note it down for each new area you will be measuring.

The applied geoid height in the app is based on a global model, a regional or national model can provide a more accurate geoid height. When processing your data, you can apply an ellipsoid height of a regional or national model. A repository of regional models can be found here: http://www.isgeoid.polimi.it/Geoid/geoid_rep.html.

7.9 Using an external base station

As mentions in Chapter 3 'Base station' it is possible to use another base station than your own. When operating in the Netherlands it will be possible to use one of the openly accessible base stations of the TU Delft, the locations of these base stations can be seen on Figure 8. These can be accessed by selecting one station from the address: 'gnss1.tudelft.nl' on port: 2101. An overview with all the base stations of TU Delft can be found here: <http://monitor.use-snip.com/?hostUrl=gnss1.tudelft.nl&port=2101>. **When using one of these base stations, make sure you select one which end with a 0 instead of a 1 (e.g. KOS100NLD0 instead of KOS100NLD1). The base stations with names which end with a 1 do not have the correct message format.**

When outside the Netherlands, the base stations of rtk2go.com could be an option. These base stations are of other rtk2go users and are openly/freely available. Since the base stations are from other users the availability of the stations relies on where and when the main user turns on their station. The current active base stations can be found here: <http://69.75.31.235:2101/SNIP::STATUS>. **NOTE: the quality and the exact location of these base stations are not indicated.**

There is also an overview of base station providers (mainly EU and USA/CAN) in the following link: <http://rtcm-ntrip.org/home.html>. Some of these casters offer the use of their base stations for free others ask for a payment. Check this before usage.

RTK2go.com

The NTRIP server for this manual is provided through the rtk2go NTRIP caster. It is possible to register a base station at this platform for free (for 2 or more registrations under the same name there will be asked for a donation). Other rtk2go users are also able to use the base station when it is connected. The base station used for this manual is registered with the following data:
MountPt name is: Base_FW_WAG (this is case sensitive and must match to be used)

- Password: hwpX8WrD (also case sensitive)
- Other details [Wageningen, NLD]
- Email: myke.koopmans@wur.nl

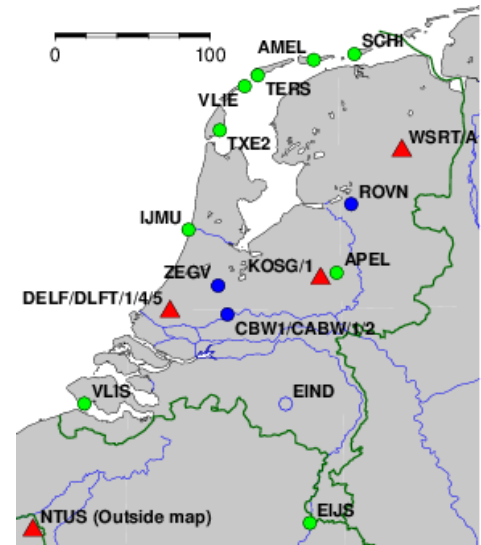
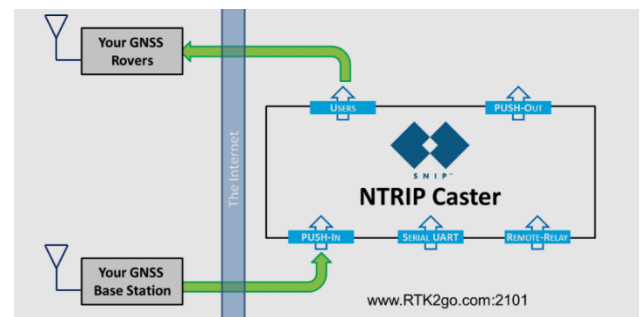


Figure 8 The locations of the base stations of TU Delft. Source: <http://gnss1.tudelft.nl/dpga/>

Figure 8 The locations of the base stations of TU Delft. Source: <http://gnss1.tudelft.nl/dpga/>



This one is for Wageningen and surroundings. When using the RTK system somewhere else a new base station registration is advised. The registration can be made at <http://www.rtk2go.com/new-reservation/>
NOTE: If you are sending wrong or imprecise data it is possible that you get banned (temporarily or permanently, depending on the frequency). Therefore, try to limit indoor test or situations which will result in poor quality data.

7.10 Changes in the configurations

The boards are pre-configured, one as base station and the other one as rover (indicated on the bottom of the boards). So, in principle no changes in configuration are needed when using them with this intention. However, when you want to make changes or want to have some more technical background information, this GitHub page could be useful: https://github.com/hcwinsemius/RTK_GNSS. Especially 'A detailed guideline for developers'.